MODEL REDUCTION AND FLUCTUATION RESPONSE IN TWO-TIMESCALE SYSTEMS

BY

MARC PIERRE KJERLAND
B.S. (University of Minnesota, Twin Cities) 2005

THESIS

Submitted in partial fulfillment of the requirements
for the degree of Doctor of Philosophy in Mathematics
in the Graduate College of the
University of Illinois at Chicago, 2015

Chicago, Illinois

In loving memory of

Elyse Mary Stern

ACKNOWLEDGMENTS

I wish to thank my advisor, Rafail Abramov, for his insights, guidance, and contributions towards the completion of this document. I deeply thank my committee, David Nicholls, Jan Verschelde, Cheng Ouyang, and Ning Ai, for their comments, support, and patience throughout this process. The staff of the Department of Mathematics, Statistics, and Computer Science (MSCS) have been consistently wonderful; they along with countless UIC graduate students have made this process infinitely more enjoyable.

This work would not have been possible without financial support from Rafail, Ning, Irina Nenciu, and MSCS. Much of this work was done through funding from the National Science Foundation (NSF) CAREER grant DMS-0845760. Thanks also to the Mathematics and Climate Research Network and other NSF-funded institutions such as IPAM, IMA, and MRSI, for providing many rewarding opportunities and personal connections.

Of course I'd like to thank my parents, Maryse Tributsch and Dean Kjerland, for everything they've done. Eternal thanks to Janice Lim for putting up with me over the past few years. Finally, thanks to all the lovely people in Chicago who continue to inspire me.

TABLE OF CONTENTS

TABLE OF CONTENTS (Continued)

CHAPTER **PAGE**

LIST OF ABBREVIATIONS

ODE	Ordinary Differential Equation
PDE	Partial Differential Equation
FDT	Fluctuation-Dissipation Theorem
DDF	Distribution Density Function

We use the convention that variables denoting vectors will be bold and typically lowercase, and matrix variables will be capitalized without other emphasis.

SUMMARY

The purpose of this work is to study an application of the averaging method for the model reduction of chaotic two-timescale systems of ordinary differential equations. We focus on two practical implementations of the averaging method: first a simple implementation averaging with respect to a single invariant measure, then a second implementation which includes a linear response closure term derived from the fluctuation-dissipation theorem. Particular emphasis is placed on the ability of the reduced systems to capture the long-time statistics and ensemble perturbation response of the slow variables in the full system, which is not guaranteed by the averaging formalism. We present some theory in the general case regarding criteria for the similarity of the perturbation responses, then these methods are applied to a Lorenz 96 system for linear and higher-order coupling between slow and fast systems. From these numerical experiments we show that the addition of the linear response closure term greatly improves the reduced model's accuracy in capturing the dynamical and statistical behavior of the full system and could be useful in practice in the presence of computational constraints.

CHAPTER 1

INTRODUCTION

From observations and first principles the scientific community has been very successful in deriving models of physical, biological, and behavioral phenomena, and while there is much to be said about intrinsic elegance or scholarly interest of such models, sometimes these model can even be useful. However, an important challenge in contemporary scientific modeling is that despite the vast amount of knowledge of the behavior of components of our world, in some cases to painstaking depth and rigor, our understanding of how these components function together as a whole is often lacking. Scientific computation represents the third component of modern scientific pursuit in addition to theory and laboratory experimentation, but even with state-of-the-art computers and numerical methods solving complex models on multiple scales of space and time can still be challenging.

In neuroscience, the Hodgkin-Huxley model for the action potential of a neuron is a highly celebrated result based on rigorous study of the squid giant axon. However, the model represents each neuron with a system of four nonlinear ODEs evolving on slow and fast timescales, making direct simulation of large network of neurons very challenging. In fluid dynamics, the Navier-Stokes equations describe the general problem of fluid motion almost too well, and the direct application of the nonlinear PDE is rarely tractable for simulations large in space or time. In geoscience, numerical weather prediction and climate forecasting consist of a dynamical core coupled with fine-scale models of biological, chemical, and physical phenomena overlaid on a

discretized earth. The scale of the application dictates which features can be resolved, as a full earth system would be impossible. In each of these cases practical implementation typically requires a reduced model derived by taking some simplifying assumptions, asymptotic limits, or truncated discretizations.

An essential question in modeling is to know how well a mathematical model represents the actual phenomenon to be understood. Perhaps a less ambitious question is to know how well a reduced model represents the full model from which it is derived in order to justify the simplifying assumptions. We make no claims to tackle such general problems in this work. However, the purpose of this work will be to study a model reduction method for two-timescale system of ODEs satisfying some assumptions so that long-term projections can be made with relative accuracy and minimal computational effort.

In this work we will describe a dimension reduction method for the slow dynamics of a two-timescale ODE system based on an averaging formalism, where the coupled fast dynamical variables are replaced with a simple deterministic process which depends on the state of the slow variables. We will apply the fluctuation-dissipation theorem, a result from statistical physics, to develop a closure approximation to the coupled fast variables which incorporates a response term appropriate to the coupling term.

We will explore the dynamical and statistical properties of these reduced systems, including criteria for validity of these approximations and numerical results in an application to a two-timescale toy model from geophysics, the Lorenz 96 system, in chaotic and quasi-periodic parameter regimes.

In Chapter 2 we begin with basic concepts and definitions for ODEs and nonlinear dynamics. In Chapter 3 we describe the theory of linear response to small perturbations in ODE systems as well as historical background of the fluctuation-dissipation theorem. In Chapter 4 we describe the problem of the two-timescale ODE system, where we have an explicit timescale separation of variables represented by a small parameter ε. We describe the averaging method for two-timescale ODEs and present two practical implementations. In 5 we discuss the criteria for an averaged model for slow variables to have similar perturbation response to the full model. The Lorenz 96 model will be introduced in Chapter 6 along with some variations whose properties will be useful in our applications and analysis. Statistical comparisons of the full and reduced Lorenz 96 models are presented in Chapter 7 and comparisons of perturbation response are presented in Chapter 8. Finally, an idealized linear response operator is discussed in Chapter 9 and we conclude.

CHAPTER 2

PRELIMINARIES - *LA MISE EN PLACE*

To begin we'll establish some definitions and concepts for ODEs and some results from linear response theory. We will rely heavily on these results in Chapter 4.

2.1 Ordinary Differential Equations

Consider the dynamical system for $\boldsymbol{x} \in \mathbb{R}^N$ given by the autonomous ODE system

$$\begin{aligned} \frac{\mathrm{d}\boldsymbol{x}}{\mathrm{d}t} &= \boldsymbol{F}(\boldsymbol{x}), \\ \boldsymbol{x}(0) &= \boldsymbol{x}_0, \end{aligned} \tag{2.1}$$

where $\boldsymbol{F} : \mathbb{R}^N \to \mathbb{R}^N$ is a differentiable vector field, and let $\phi^t : \mathbb{R}^N \to \mathbb{R}^N$ be the flow generated by $\boldsymbol{F}$, a one-parameter family of transformations which solves the initial value problem

$$\begin{aligned} \frac{\mathrm{d}\phi^t(\boldsymbol{x})}{\mathrm{d}t} &= \boldsymbol{F}(\phi^t(\boldsymbol{x})), \\ \phi^0(\boldsymbol{x}) &= \boldsymbol{x}, \end{aligned} \tag{2.2}$$

and which notably has the group property $\phi^s \circ \phi^t = \phi^{s+t}$. For most of this work we will drop the parantheses and use the notation $\phi^t\boldsymbol{x}$ to denote the flow on $\boldsymbol{x}$.

We say that a set A is *invariant* under the flow if $\phi^t(A) = A$ for all t, and a measure μ is invariant if $\mu(\phi^t(A)) = \mu(A)$ for any measurable set A and any time t. An invariant probability measure μ is said to be *ergodic* if

$$\phi^t A = A \quad \Rightarrow \quad \mu(A) = 0 \text{ or } \mu(A) = 1 \text{ or } t = 0. \tag{2.3}$$

In this work we primarily concern ourselves with systems which have ergodic invariant probability measures, and here we make precise when this is the case.

A compact ϕ-invariant set $\Lambda \in \mathbb{R}^N$ is known as an *attractor* if there is a neighborhood U of Λ such that for all $\boldsymbol{x} \in U$, $\phi^t \boldsymbol{x} \to \Lambda$ as $t \to \infty$. An attractor is irreducible if it cannot be written as the union of two disjoint attractors. Given the differential $D\phi$, an attractor Λ is said to be *hyperbolic* if the tangent space for every $\boldsymbol{x} \in \Lambda$ admits a continuous splitting into $E^s_{\boldsymbol{x}} \oplus E^u_{\boldsymbol{x}}$ where $E^s_{\boldsymbol{x}}$ and $E^u_{\boldsymbol{x}}$ are $D\phi$-invariant subspaces such that there exist constants $c > 0$ and $0 < \theta < 1$ where

$$\begin{aligned} \|D\phi^t u\| &\leq c\theta^t \|u\|, \quad \forall u \in E^s, t > 0, \\ \|D\phi^{-t} v\| &\leq c\theta^t \|v\|, \quad \forall v \in E^u, t > 0. \end{aligned} \tag{2.4}$$

If an attractor Λ is irreducible, hyperbolic, and compact, and has a dense set of periodic points, it is known as an Axiom A attractor, and there exists a unique ϕ-invariant Borel probability measure μ on Λ such that for any continuous observable function $\boldsymbol{b}(\boldsymbol{x})$ we have, for Lebesgue-almost-every $\boldsymbol{x}$,

$$\lim_{S \to \infty} \frac{1}{S} \int_0^S \boldsymbol{b}(\phi^s \boldsymbol{x}) \, \mathrm{d}s \to \int \boldsymbol{b} \, \mathrm{d}\mu. \tag{2.5}$$

In general this invariant measure, known as the Sinai-Ruelle-Bowen (SRB) measure, will not be absolutely continuous with respect to the Lebesgue measure. If this system has a nontrivial unstable subspace E^u we call it *chaotic* (1).

We will mostly be considering dynamical systems that are mixing, so that for any pair of square-integrable functions $f, g \in L^2(\mu)$ we have:

$$\lim_{t\to\infty} \int f \cdot \left(g \circ \phi^t\right) \, \mathrm{d}\mu = \int f \, \mathrm{d}\mu \cdot \int g \, \mathrm{d}\mu \tag{2.6}$$

This is a stronger assumption than ergodicity. For such systems, a typical long-time solution "forgets" its initial state. Numerically, the equality of time average and space average (Equation 2.5) provides the particularly useful property that large ensemble statistics can be interchanged with long-time statistics of a single trajectory.

2.2 Tangent map

We define the tangent map as

$$T^t_{\boldsymbol{x}_0} := \left.\frac{\partial \phi^t(\boldsymbol{x})}{\partial \boldsymbol{x}}\right|_{\boldsymbol{x}_0}. \tag{2.7}$$

Differentiating (Equation 2.1) with respect to $\boldsymbol{x}$, we have

$$\begin{aligned} \frac{\partial}{\partial t} T^t_{\boldsymbol{x}} &= J_{\boldsymbol{F}}(\phi^t \boldsymbol{x}) T^t_{\boldsymbol{x}} \\ T^0_{\boldsymbol{x}} &= \mathrm{Id}_N, \end{aligned} \tag{2.8}$$

where $J_{\boldsymbol{F}}(\boldsymbol{x})$ is the Jacobian matrix of $\boldsymbol{F}$ at $\boldsymbol{x}$ and Id_N is the $N \times N$ identity matrix, whose solution is given by

$$T^t_{\boldsymbol{x}} = \exp\left(\int_0^t J_{\boldsymbol{F}}(\phi^s \boldsymbol{x})\,\mathrm{d}s\right). \tag{2.9}$$

Note that the tangent map has the property $T^{s+t}_{\boldsymbol{x}} = T^s_{\phi^t \boldsymbol{x}} T^t_{\boldsymbol{x}}$, found by applying the chain rule of differentiation to the identity $\phi^{s+t} = \phi^s \circ \phi^t$.

2.3 Lyapunov exponent

The largest Lyapunov exponent characterizes the average rate of separation of infinitesimally close trajectories and hence the predictability of the system. It is given by

$$\lambda_1 := \lim_{t\to\infty} \lim_{\boldsymbol{x}_1 \to \boldsymbol{x}_0} \frac{1}{t} \ln \frac{\|\phi^t \boldsymbol{x}_1 - \phi^t \boldsymbol{x}_0\|}{\|\boldsymbol{x}_1 - \boldsymbol{x}_0\|}, \tag{2.10}$$

with $\|\cdot\|$ the standard Euclidean norm. For an ergodic system, Osledec's theorem guarantees existence of this limit and equality for almost-every $\boldsymbol{x}$. The full Lyapunov spectrum can be defined but we will only refer to the largest, simply as *the* Lyapunov exponent. A strongly chaotic system has a positive Lyapunov exponent, characterizing the exponential sensitivity to initial conditions: $\|\phi^t(\boldsymbol{x}) - \phi^t(\boldsymbol{x} + \delta\boldsymbol{x})\| \approx e^{\lambda_1 t}\|\delta\boldsymbol{x}\|$ as $\delta\boldsymbol{x} \to 0$ (2). Definitions of weak chaos generally refer to systems where divergence of nearby solutions is sub-exponential but positive.

The Lyapunov exponents are closely related to the tangent map. If we define

$$L(\boldsymbol{x}) = \lim_{t\to\infty} \left(T^t_{\boldsymbol{x}} (T^t_{\boldsymbol{x}})^T\right)^{1/2t}, \tag{2.11}$$

which by Osledec's theorem will be equal for almost any initial state $\boldsymbol{x}$, with eigenvalues $\Lambda_1 \geq \Lambda_2 \geq \ldots \geq \Lambda_N$, the Lyapunov exponents are given by

$$\lambda_i = \log \Lambda_i. \tag{2.12}$$

2.4 The Kolmogorov equations

Two important equations for ODEs are the Kolmogorov backward and forward equations which we describe here.

Note that if $\phi^t \boldsymbol{x}$ solves (Equation 2.1) and if $V \in C^1$ then

$$\frac{\mathrm{d}}{\mathrm{d}t}\left(V(\phi^t \boldsymbol{x})\right) = \nabla V(\phi^t \boldsymbol{x}) \cdot F(\phi^t \boldsymbol{x}) \tag{2.13}$$

Consider then the generator $\mathcal{L}$, a linear operator which for any $v \in C^1$ is given by

$$\mathcal{L}v = \boldsymbol{F} \cdot \nabla v, \tag{2.14}$$

and the following Cauchy problem for $v(\boldsymbol{x}, t)$,

$$\begin{aligned} &\frac{\partial v}{\partial t} = \mathcal{L}v, \quad \text{for } (\boldsymbol{x}, t) \in \mathbb{R}^N \times (0, \infty), \\ &v(\boldsymbol{x}, 0) = v_0(\boldsymbol{x}), \quad \text{for } \boldsymbol{x} \in \mathbb{R}^N. \end{aligned} \tag{2.15}$$

also known as the Kolmogorov backward equation.When v_0 is sufficiently smooth so that (Equation 2.15) has a classical solution, that solution will be given by

$$v(\boldsymbol{x}, t) = v_0(\phi^t \boldsymbol{x}), \quad \forall t \in \mathbb{R}^+, \boldsymbol{x} \in \mathbb{R}^N, \tag{2.16}$$

since $v(\boldsymbol{x}, 0) = v_0(\boldsymbol{x})$ and by the identity in (Equation 2.13).

More generally, for a bounded operator $\mathcal{L}$ we can define the semigroup

$$e^{\mathcal{L}t} := \sum_{k=0}^{\infty} \frac{t^k \mathcal{L}^k}{k!}, \tag{2.17}$$

with $e^{\mathcal{L}0} = \mathrm{Id}$, so that $v(\boldsymbol{x}, t) = (e^{\mathcal{L}t} v_0)(\boldsymbol{x})$ solves the general Cauchy problem for $\mathcal{L}$, (Equation 2.15).

If we extend the definition of the operator $e^{\mathcal{L}t}$ to act on arbitrary functions $v \in L^\infty$ as

$$\left(e^{\mathcal{L}t} v\right)(\boldsymbol{x}) = v(\phi^t \boldsymbol{x}), \quad \forall t \in \mathbb{R}^+, \boldsymbol{x} \in \mathbb{R}^N, \tag{2.18}$$

then the infinitesimal generator $\mathcal{L}$ is defined as the following limit when it exists:

$$\mathcal{L} v = \lim_{t \to 0} \frac{e^{\mathcal{L}t} v - v}{t}. \tag{2.19}$$

If the initial condition to (Equation 2.1) is a random variable with probability density $\rho_0(\boldsymbol{x})$, the evolution of its distribution density $\rho(\boldsymbol{x}, t)$ is given by the Liouville equation,

$$\begin{aligned} &\frac{\partial \rho}{\partial t} = \mathcal{L}^* \rho, \quad \text{for } (\boldsymbol{x}, t) \in \mathbb{R}^N \times (0, \infty), \\ &\rho(\boldsymbol{x}, 0) = \rho_0(\boldsymbol{x}), \quad \text{for } \boldsymbol{x} \in \mathbb{R}^N, \end{aligned} \tag{2.20}$$

also known as the Kolmogorov forward equation. If the system is ergodic with a smooth invariant distribution density $\rho^\infty(\boldsymbol{x})$, solutions to the Liouville equation will tend to ρ^∞ as $t \to \infty$. Using the semigroup notation the solution to (Equation 2.20) is given by

$$\rho(\boldsymbol{x}, t) = (e^{\mathcal{L}^* t} \rho_0)(\boldsymbol{x}). \tag{2.21}$$

Given an Axiom A attractor with an invariant measure μ we will determine the $L^2(\mu)$-adjoint operators. Given the semigroup definition as in (Equation 2.18) and smooth functions u and v, we have

$$\begin{aligned} \langle e^{\mathcal{L} t} v, u \rangle &= \int v(\phi^t \boldsymbol{x})\, u \, \mathrm{d}\mu \\ &= \int v(\phi^t \boldsymbol{x})\, u(\boldsymbol{x}) \, \mathrm{d}\mu(\boldsymbol{x}) \\ &= \int v(\boldsymbol{x})\, u(\phi^{-t} \boldsymbol{x}) \, \mathrm{d}\mu(\boldsymbol{x}) \\ &= \langle v, e^{\mathcal{L}^* t} u \rangle, \end{aligned} \tag{2.22}$$

so that $e^{\mathcal{L}^* t} u = u \circ \phi^{-t}$. Then $\mathcal{L}^*$ is given by the following limit when it exists:

$$\begin{aligned} \mathcal{L}^* \rho &:= \lim_{t \to 0} \frac{e^{\mathcal{L}^* t} \rho - \rho}{t}. \\ &= \lim_{t \to 0} \frac{\rho \circ \phi^{-t} - \rho}{t}. \\ &= -\mathcal{L} \rho \end{aligned} \tag{2.23}$$

so we see that $\mathcal{L}$ is skew-adjoint. From the ergodicity assumption the null space of $\mathcal{L}$ is spanned by constants in $\boldsymbol{x}$. We will revisit these operators for multiscale equations in Chapter 4.

CHAPTER 3

LINEAR RESPONSE THEORY

3.1 The linear response

Suppose the system (Equation 2.1) is perturbed by adding a small forcing term $\boldsymbol{\delta F}(\boldsymbol{x}, t)$ resulting in the time-dependent system

$$\frac{\mathrm{d}\boldsymbol{x}}{\mathrm{d}t} = \boldsymbol{F}(\boldsymbol{x}) + \boldsymbol{\delta F}(\boldsymbol{x}, t), \qquad \boldsymbol{x}(t) = \hat{\phi}^t \boldsymbol{x}(0). \tag{3.1}$$

where $\boldsymbol{\delta F}(\boldsymbol{x}, t) = 0$ for $t < 0$ and where $\hat{\phi}^t$ is the flow map corresponding to this perturbed system with initial condition at $t = 0$. Many of the results in this section can be adapted to more general forms of perturbation, but in this work we will restrict ourselves to the form in Equation 3.1.

From equivalent initial conditions the trajectories of the perturbed and unperturbed systems should diverge for $t > 0$. We are interested in this perturbation response, which is dependent on the forcing in a relationship which *a priori* is unknown. However, when the forcing is small enough we expect this dependence to be approximately linear, and we will derive an approximate linear response which will hold for sufficiently small times and forcings. We will denote this response by

$$\delta\phi^t \boldsymbol{x} := \hat{\phi}^t \boldsymbol{x} - \phi^t \boldsymbol{x}, \tag{3.2}$$

with $\delta\phi^0\boldsymbol{x} = 0$.

In a real-world application, the state variables $\boldsymbol{x}$ might not be directly observable or might not be of specifical interest. Furthermore, for chaotic systems one may be more interested in ensemble statistics than in individual trajectories. Given a vector-valued observable function $\boldsymbol{b} \in L^1(\mu)$ its its mean response at time t following the perturbation $\boldsymbol{\delta F}$ is given by

$$\delta\langle \boldsymbol{b} \rangle(t) = \int \left(\boldsymbol{b}(\hat{\phi}^t \boldsymbol{x}) - \boldsymbol{b}(\phi^t \boldsymbol{x}) \right) \, \mathrm{d}\mu(\boldsymbol{x}). \tag{3.3}$$

We seek a linear response operator $\mathcal{R}$ such that

$$\delta\langle \boldsymbol{b} \rangle \approx \mathcal{R}(\boldsymbol{\delta F})(t) \tag{3.4}$$

which, in the case where the forcing is only time-dependent, $\boldsymbol{\delta F}(\boldsymbol{x}, t) = \boldsymbol{\delta f}(t)$, will take the form

$$\mathcal{R}(\boldsymbol{\delta F})(t) = \int_0^t R(t, t') \boldsymbol{\delta f}(t') \, \mathrm{d}t'. \tag{3.5}$$

3.2 Fluctuation-Dissipation Theorem

The fluctuation-dissipation theorem (FDT), also known as the fluctuation-response relation, provides an explicit connection between a system's relaxation following an external perturbation and its natural fluctuations about its mean state, provided some appropriate conditions are satisfied. An example of this phenomenon was first described at the turn of the 20th century independently by Einstein and Smoluchowski amid the search for evidence of the atomic

hypothesis. They established a relationship between the viscous friction of a moving spherical particle (given by Stokes' Law) to the fluctuation of velocities in Brownian motion (3; 4; 5; 6). A seminal 1928 paper by Nyquist at Bell Labs explained an observed relationship between random electromotive force in a conductor and the impedance of the conductor using first principles of the thermal fluctuations of electrons and an equipartition argument (7). More general treatments of the fluctuation-dissipation theorem were given by Callen and Welton (1951) and Kubo (1957), and proof of the relation is generally attributed to Kraichnan (1959) for systems with a quadratic invariant, incompressible phase volume, and sufficiently weak forcing (8; 9; 10).

In 1975 Cecil Leith at the National Center for Atmospheric Research introduced FDT to the geoscience community. The sensitivity of the earth's climate would be very useful to know since we would like to be able to anticipate the consequences of human activity or extreme natural events. However, it would be quite difficult to produce experimental evidence of the response which is larger than the climate noise. Leith proposed using the FDT as an alternative which requires only the observable fluctuations of the earth's climate to produce predictions of small perturbations response (11; 12). The FDT formulation of Kraichnan and Leith is given at the end of this chapter as (Equation 3.27), and holds for systems which satisfy the criteria of Kraichnan and whose distributions will necessarily be Gaussian.

However, earth systems such as the atmosphere are typically subject to both damping and forcing, resulting in models with a contracting phase space and no exact quadratic invariant. As a consequence the conditions of Kraichnan do not hold. However, the results of FDT have been extended to such systems as in the work of Deker & Haake (1975), Risken (1984), and Majda,

Grote, & Abramov (2005), as we shall see in the next sections (13; 14; 15). The response formula which we derive is known as the quasi-Gaussian linear response, which will hold approximately for systems whose distributions are non-Gaussian.

3.3 The Fokker-Planck equation

We will need to establish some results on the smoothness of the attracting invariant manifold μ of the unperturbed system (Equation 2.1) with respect to perturbations as in (Equation 3.1). If μ is absolutely continuous with respect to the Lebesgue measure, then there is a distribution density function $\rho(\boldsymbol{x})$ such that $\mathrm{d}\mu = \rho\,\mathrm{d}\boldsymbol{x}$. It is known that most deterministic dynamical systems do not have invariant measures satisfying this property, and instead their solutions live on strange attractors with fractal dimension which have SRB measures that are singular with respect to the Lebesgue measure (16; 17; 1). However, even a small amount of random noise is typically sufficient to ensure existence of a distribution density (18). This noise will generally be present *in vivo* due to unresolved physical processes and *in silico* in the form of small pseudorandom noise due to numerical roundoff. In particular, this noise can be small enough so as not to significantly affect the statistics of the noise-free system.

Introducing this stochastic regularization we have

$$\mathrm{d}\boldsymbol{x}_\varepsilon = \boldsymbol{F}(\boldsymbol{x}_\varepsilon)\,\mathrm{d}t + \varepsilon\,\mathrm{d}\boldsymbol{W}_t, \quad \boldsymbol{x}_\varepsilon(0) = \boldsymbol{x}_0, \tag{3.6}$$

where ε is a small positive scalar and $\boldsymbol{W}_t$ is a standard Wiener process in $\mathbb{R}^N$. Now forced by small Gaussian white noise, the evolution of a probability density $\rho_\varepsilon(t, \boldsymbol{x})$ in this system is given by the Fokker-Planck equation (14):

$$\frac{\partial \rho_\varepsilon}{\partial t} + \nabla \cdot (\boldsymbol{F}\rho_\varepsilon) = \frac{\varepsilon}{2}\Delta\rho_\varepsilon, \tag{3.7}$$

where Δ is the Laplacian operator. When $\varepsilon = 0$ this is equivalent to the Liouville equation (Equation 2.20). For $\boldsymbol{F}$ corresponding to an ergodic system, the Fokker-Planck equation will have a unique stationary solution $\rho_\varepsilon^\infty(\boldsymbol{x})$ (18).

Now we can consider the effect of the perturbation on the equilibrium distribution. The Fokker-Planck equation for the corresponding regularized perturbed system is given by:

$$\begin{aligned} &\frac{\partial \rho_\varepsilon^{\boldsymbol{\delta F}}}{\partial t} + \nabla \cdot ((\boldsymbol{F} + \boldsymbol{\delta F})\rho_\varepsilon^{\boldsymbol{\delta F}}) = \frac{\varepsilon}{2}\Delta\rho_\varepsilon^{\boldsymbol{\delta F}}, \\ &\rho_\varepsilon^{\boldsymbol{\delta F}}(0, \boldsymbol{x}) = \rho_\varepsilon^\infty(\boldsymbol{x}). \end{aligned} \tag{3.8}$$

Using this interpretation, the mean response of an observable function $b \in L^1$ at time t following the onset of the perturbation $\boldsymbol{\delta F}$ is given by

$$\delta\langle b\rangle(t) := \int b(\boldsymbol{x})\rho_\varepsilon^{\boldsymbol{\delta F}}(t, \boldsymbol{x})\,\mathrm{d}\boldsymbol{x} - \int b(\boldsymbol{x})\rho_\varepsilon^\infty(\boldsymbol{x})\,\mathrm{d}\boldsymbol{x}. \tag{3.9}$$

In the next section we will derive a linear response formula to approximate this expression.

3.4 Derivation of the linear response operator

If we subtract (Equation 2.1) from (Equation 3.1), and if $\boldsymbol{\delta F}$ is differentiable with we have

$$\begin{aligned}\frac{\partial}{\partial t}\delta\phi^t\boldsymbol{x} &= \boldsymbol{F}(\hat{\phi}^t\boldsymbol{x}) - \boldsymbol{F}(\phi^t\boldsymbol{x}) + \boldsymbol{\delta F}(\hat{\phi}^t\boldsymbol{x}, t),\\ &= J_{\boldsymbol{F}}(\phi^t\boldsymbol{x})\delta\phi^t\boldsymbol{x} + \boldsymbol{\delta F}(\phi^t\boldsymbol{x}, t) + J_{\boldsymbol{\delta F}}(\phi^t\boldsymbol{x})\delta\phi^t\boldsymbol{x} + \mathcal{O}(\|\delta\phi^t\boldsymbol{x}\|^2),\end{aligned} \tag{3.10}$$

where $J_{\boldsymbol{F}}$ and $J_{\boldsymbol{\delta F}}$ are the Jacobian matrices of $\boldsymbol{F}$ and $\boldsymbol{\delta F}$, respectively. If $\boldsymbol{\delta F}$ has a small first derivatives, we can neglect the last two terms to get the following initial value problem:

$$\begin{aligned}\frac{\partial}{\partial t}\delta\phi^t\boldsymbol{x} &= J_{\boldsymbol{F}}(\phi^t\boldsymbol{x})\delta\phi^t\boldsymbol{x} + \boldsymbol{\delta F}(\phi^t\boldsymbol{x}, t)\\ \delta\phi^0\boldsymbol{x} &= 0.\end{aligned} \tag{3.11}$$

The solution to this linear ODE is given by Duhamel's principle:

$$\delta\phi^t\boldsymbol{x} = \int_0^t \exp\left(\int_\tau^t J_{\boldsymbol{F}}(\phi^s\boldsymbol{x})\,\mathrm{d}s\right)\boldsymbol{\delta F}(\phi^\tau\boldsymbol{x}, \tau)\,\mathrm{d}\tau. \tag{3.12}$$

Recalling the definition of the tangent map, we note that the initial value problem

$$\begin{aligned}\frac{\partial}{\partial t}T^{t-\tau}_{\phi^\tau\boldsymbol{x}} &= J_{\boldsymbol{F}}(\phi^t\boldsymbol{x})T^{t-\tau}_{\phi^\tau\boldsymbol{x}},\\ T^0_{\phi^\tau\boldsymbol{x}} &= \mathrm{Id}_N,\end{aligned} \tag{3.13}$$

found by multiplying both sides of (Equation 2.8) by $T^{-\tau}_{\phi^\tau\boldsymbol{x}}$, has solution

$$T^{t-\tau}_{\phi^\tau\boldsymbol{x}} = \exp\left(\int_\tau^t J_{\boldsymbol{F}}(\phi^s\boldsymbol{x})\,\mathrm{d}s\right). \tag{3.14}$$

Plugging this into (Equation 3.12) we have

$$\delta\phi^t \boldsymbol{x} = \int_0^t T^{t-\tau}_{\phi^\tau \boldsymbol{x}} \boldsymbol{\delta F}(\phi^\tau \boldsymbol{x}, \tau)\, \mathrm{d}\tau. \tag{3.15}$$

Linearizing the mean response of an observable $\boldsymbol{b} \in L^1(\mu) \cap C^1$, as in (Equation 3.3), we have

$$\delta\langle \boldsymbol{b} \rangle(t) \approx \int J_{\boldsymbol{b}}(\phi^t \boldsymbol{x}) \delta\phi^t \boldsymbol{x}\, \mathrm{d}\mu(\boldsymbol{x}) \tag{3.16}$$

where $J_{\boldsymbol{b}}(\phi^t \boldsymbol{x})$ is the Jacobian of $\boldsymbol{b}$ at $\phi^t \boldsymbol{x}$. From (Equation 3.15) we have

$$\begin{aligned} \delta\langle \boldsymbol{b} \rangle(t) &= \int_0^t \int J_{\boldsymbol{b}}(\phi^t \boldsymbol{x}) T^{t-\tau}_{\phi^\tau \boldsymbol{x}} \boldsymbol{\delta F}(\phi^\tau \boldsymbol{x}, \tau)\, \mathrm{d}\mu(\boldsymbol{x})\, \mathrm{d}\tau \\ &= \int_0^t \int J_{\boldsymbol{b}}(\phi^{t-\tau} \boldsymbol{x}) T^{t-\tau}_{\boldsymbol{x}} \boldsymbol{\delta F}(\boldsymbol{x}, \tau)\, \mathrm{d}\mu(\boldsymbol{x})\, \mathrm{d}\tau, \end{aligned} \tag{3.17}$$

where the second equality is due to the invariance of μ under ϕ^t. Thus we have the linear response relation

$$\delta\langle \boldsymbol{b} \rangle(t) = \int_0^t \int \nabla_x \left(\boldsymbol{b}(\phi^{t-\tau} \boldsymbol{x}) \right) \boldsymbol{\delta F}(\boldsymbol{x}, \tau)\, \mathrm{d}\mu(\boldsymbol{x})\, \mathrm{d}\tau. \tag{3.18}$$

From the ergodic hypothesis, this is equivalent to the time average:

$$\delta\langle \boldsymbol{b} \rangle(t) = \lim_{S \to \infty} \frac{1}{S} \int_0^t \int_0^S \nabla_x \left(\boldsymbol{b}(\phi^{t-\tau+s} \boldsymbol{x}) \right) \boldsymbol{\delta F}(\phi^s \boldsymbol{x}, \tau)\, \mathrm{d}s\, \mathrm{d}\tau. \tag{3.19}$$

See also (19; 20; 21; 22; 23; 24).

The tangent map $T_{\boldsymbol{x}}^t$ in (Equation 3.17) can be numerically computed in tandem with a solution trajectory $\boldsymbol{x}(t)$, using for example a Runge-Kutta scheme for which the derivation is straightforward. However, in practice (Equation 3.18) is difficult to compute for large nonlinear systems, which is often the case in geophysical applications. Numerical integration of the tangent map requires multiplication of $N \times N$ matrices at each Runge-Kutta step which greatly increases the computational cost. A further complication arises for systems with positive Lyapunov exponents which introduce numerical instability in the tangent map computation. Due to these factors, the usefulness of the tangent map for linear response prediction is restriced to short time horizons. However, if we make some simplifying assumptions about the invariant distribution we can derive an alternative linear response formula which is much easier to implement in practice.

3.5 Quasi-Gaussian linear response

Assuming existence of a smooth invariant distribution $\mathrm{d}\mu = \rho \, \mathrm{d}\boldsymbol{x}$, integrating by parts in (Equation 3.18) we have

$$\delta\langle \boldsymbol{b} \rangle(t) = -\int_0^t \int_{\mathbb{R}^N} \boldsymbol{b}(\phi^{t-\tau}\boldsymbol{x}) \, \nabla_x \cdot (\boldsymbol{\delta F}(\boldsymbol{x},\tau)\rho(\boldsymbol{x})) \, \mathrm{d}\boldsymbol{x} \, \mathrm{d}\tau. \tag{3.20}$$

Now let us write the distribution density as $\rho(\boldsymbol{x}) = e^{-q(\boldsymbol{x})}$, where q is a differentiable function which goes to infinity as $|\boldsymbol{x}| \to \infty$. Then we have

$$\begin{aligned}\delta\langle \boldsymbol{b}\rangle(t) &= \int_0^t \int_{\mathbb{R}^N} \boldsymbol{b}(\phi^{t-\tau}\boldsymbol{x}) \left(\nabla_x q(\boldsymbol{x}) \cdot \boldsymbol{\delta F}(\boldsymbol{x},\tau) - \nabla_x \cdot \boldsymbol{\delta F}(\boldsymbol{x},\tau)\right) e^{-q(\boldsymbol{x})} \,\mathrm{d}\boldsymbol{x}\,\mathrm{d}\tau \\ &= \int_0^t \int \boldsymbol{b}(\phi^{t-\tau}\boldsymbol{x}) \left(\nabla_x q(\boldsymbol{x}) \cdot \boldsymbol{\delta F}(\boldsymbol{x},\tau) - \nabla_x \cdot \boldsymbol{\delta F}(\boldsymbol{x},\tau)\right) \,\mathrm{d}\mu(\boldsymbol{x})\,\mathrm{d}\tau.\end{aligned} \tag{3.21}$$

If we make the simplifying assumption that $\rho(\boldsymbol{x})$ is a Gaussian distribution with mean $\overline{\boldsymbol{x}}$ and covariance matrix Σ, that is,

$$\rho(\boldsymbol{x}) = \frac{\exp\left(-\frac{1}{2}(\boldsymbol{x}-\overline{\boldsymbol{x}})^T\Sigma^{-1}(\boldsymbol{x}-\overline{\boldsymbol{x}})\right)}{\sqrt{(2\pi)^N|\Sigma|}} \tag{3.22}$$

then we have the so-called quasi-Gaussian linear response approximation

$$\begin{aligned}\delta\langle \boldsymbol{b}\rangle(t) &\approx \int_0^t \int \boldsymbol{b}(\phi^{t-\tau}\boldsymbol{x}) \left((\boldsymbol{x}-\overline{\boldsymbol{x}})^T\Sigma^{-1}\boldsymbol{\delta F}(\boldsymbol{x},\tau) - \nabla_x \cdot \boldsymbol{\delta F}(\boldsymbol{x},\tau)\right) \,\mathrm{d}\mu(\boldsymbol{x})\,\mathrm{d}\tau. \\ &= \lim_{S\to\infty} \frac{1}{S} \int_0^t \int_0^S \boldsymbol{b}(\boldsymbol{x}(s+t-\tau) \left((\boldsymbol{x}(s)-\overline{\boldsymbol{x}})^T\Sigma^{-1}\boldsymbol{\delta F}(\boldsymbol{x}(s),\tau) - \nabla_x \cdot \boldsymbol{\delta F}(\boldsymbol{x}(s),\tau)\right) \,\mathrm{d}s\,\mathrm{d}\tau,\end{aligned} \tag{3.23}$$

with $\overline{\boldsymbol{x}}$ and Σ denoting the sample mean and covariance:

$$\begin{aligned}\overline{\boldsymbol{x}} &= \lim_{S\to\infty} \frac{1}{S} \int_0^S \boldsymbol{x}(s)\,\mathrm{d}s \\ \Sigma &= \lim_{S\to\infty} \frac{1}{S} \int_0^S \boldsymbol{x}(s)\left(\boldsymbol{x}(s)-\overline{\boldsymbol{x}}\right)^T \,\mathrm{d}s.\end{aligned} \tag{3.24}$$

In practice (Equation 3.23) is simple to compute, requiring only a sufficiently long trajectory in the unperturbed system, and is useful in chaotic mixing systems. (11; 19; 20; 21; 22; 23; 15; 14).

In the case where the perturbation is only time-dependent, $\boldsymbol{\delta F}(\boldsymbol{x}, t) = \boldsymbol{\delta f}(t)$, and where the observed quantity of interest is the state variable itself, $\boldsymbol{b}(\boldsymbol{x}) = \boldsymbol{x}$, the formula simplifies greatly. Defining the lag covariance as

$$\Sigma(t) = \lim_{S\to\infty} \frac{1}{S} \int_0^S \boldsymbol{x}(s+t) \left(\boldsymbol{x}(s) - \overline{\boldsymbol{x}}\right)^T \mathrm{d}s \tag{3.25}$$

and the autocorrelation function as

$$C(t) = \Sigma(t)\Sigma(0)^{-1}. \tag{3.26}$$

then the quasi-Gaussian response of the mean state of $\boldsymbol{x}$ is given by

$$\boldsymbol{\delta}\overline{\boldsymbol{x}}(t) = \int_0^t C(t-\tau)\boldsymbol{\delta f}(\tau)\, \mathrm{d}\tau. \tag{3.27}$$

This is the fluctuation-dissipation result for linear response presented in Kraichnan (1957) and Leith (1975), and will hold exactly for the systems they considered which necessarily have Gaussian distribution. For systems with non-Gaussian distributions, (Equation 3.27) will be an approximation to the linear response.(10; 11; 25)

3.6 Applications of the fluctuation-dissipation theorem

Several authors have applied the FDT to problems in geoscience. Bell (1980) tested Leith's FDT on a truncated model of the barotropic vorticity equation and pushed it further by adding viscosity and forcing to the model so that energy and enstrophy were no longer conserved.

Langen and Alexeev (2005) use the FDT to estimate the response of a sophisticated atmospheric general circulation model (AGCM) to doubling of atmospheric CO_2. Gritsun and Branstator tested response to spatially localized heat forcing in an AGCM, and further tested the skill of the inverse problem estimating the forcing needed to produce a given response. In each of these cases the FDT provided effective predictions, although the authors working with AGCMs note the practical difficulties in estimating the covariance matrix for such large systems.(25; 26; 27)

In the next chapter we will apply the FDT to a different type of application, where we seek structural changes of invariant manifolds due to small changes in parameters, at least as observed by projections onto simple functions.

CHAPTER 4

AVERAGED SLOW DYNAMICS FOR A TWO-TIMESCALE SYSTEM

4.1 Averaging method for two-timescale systems

Consider a general two-timescale dynamical system with slow variables $\boldsymbol{x} \in \mathbb{R}^{N_x}$ and fast variables $\boldsymbol{y} \in \mathbb{R}^{N_y}$:

$$\begin{aligned} \frac{\mathrm{d}\boldsymbol{x}}{\mathrm{d}t} &= \boldsymbol{F}(\boldsymbol{x}, \boldsymbol{y}), \\ \frac{\mathrm{d}\boldsymbol{y}}{\mathrm{d}t} &= \frac{1}{\varepsilon}\boldsymbol{G}(\boldsymbol{x}, \boldsymbol{y}), \\ \boldsymbol{x}(0) &= \boldsymbol{x}_0, \quad \boldsymbol{y}(0) = \boldsymbol{y}_0, \end{aligned} \tag{4.1}$$

where $\boldsymbol{F}$ and $\boldsymbol{G}$ are differentiable vector fields and $\varepsilon \ll 1$ is a scale separation parameter.

The $\boldsymbol{y}$-variables might represent some subgrid-scale or microscopic process, or perhaps $\boldsymbol{x}$ and $\boldsymbol{y}$ represent analogous processes with different physical parameters. From a numerical standpoint, computing a multiscale system with large timescale separation using an explicit numerical method typically requires a very small timestep discretization. Furthermore, we might also expect the number of fast variables to be large, $N_y \gg N_x$, which is likely to prohibit implicit numerical methods that could otherwise accommodate larger timesteps. In any case, for many real-world applications the fully-resolved multiscale model is simply intractable, and an appropriate reduced model will be needed to perform a long-term projection.

In this chapter we will derive a reduced model for the slow dynamics of the multiscale system using properties of the invariant distribution of the fast variables. This reduced model

will provide approximate solutions of the multiscale system originating from the same initial conditions for times up to $t = \mathcal{O}(1)$ as $\varepsilon \to 0$. The solutions will also be appropriately close in the long-time statistics. Formal theory for closeness of solutions is presented in this chapter and experimental evidence for statistical similarity will be presented in Chapter 7. Criteria for similarity of perturbation response will be derived in Chapter 5 and comparisons of actual response will be shown in Chapter 8.

If we consider the change of variables $\tau = \varepsilon t$ to switch to the fast time scale, we have

$$\begin{aligned} \frac{\mathrm{d}\boldsymbol{x}}{\mathrm{d}\tau} &= \varepsilon \boldsymbol{F}(\boldsymbol{x}, \boldsymbol{y}), \\ \frac{\mathrm{d}\boldsymbol{y}}{\mathrm{d}\tau} &= \boldsymbol{G}(\boldsymbol{x}, \boldsymbol{y}), \\ \boldsymbol{x}(0) &= \boldsymbol{x}_0, \quad \boldsymbol{y}(0) = \boldsymbol{y}_0, \end{aligned} \tag{4.2}$$

In the limiting case $\varepsilon \to 0$, or for sufficiently small time, $\boldsymbol{x}$ will be approximately constant and the fast dynamics are given by the *fast limiting system*

$$\begin{aligned} \frac{\mathrm{d}\boldsymbol{z}}{\mathrm{d}\tau} &= \boldsymbol{G}(\boldsymbol{x}, \boldsymbol{z}) \\ \boldsymbol{z}(0) &= \boldsymbol{y}_0, \end{aligned} \tag{4.3}$$

with flow operator $\varphi^t_{\boldsymbol{x}}$ and invariant probability measure μ_x, parametrized by $\boldsymbol{x}$. We will assume the fast limiting system (Equation 4.3) is mixing (and consequently ergodic) at least for values of $\boldsymbol{x}$ on some relevant subset of $\mathbb{R}^{N_x}$. In particular, we will need its lag covariance (Equation 3.25) to decay sufficiently fast so that $\int_0^\infty \Sigma_\xi(s)\,\mathrm{d}s$ is finite.

If we define the vector field

$$\overline{\boldsymbol{F}}(\boldsymbol{x}) := \int \boldsymbol{F}(\boldsymbol{x}, \boldsymbol{y}) \, \mathrm{d}\mu_x(\boldsymbol{y}) \tag{4.4}$$

we will show that the evolution for the slow variables $\boldsymbol{x}(t)$ in the multiscale system (Equation 4.1) can be approximated by solving

$$\begin{aligned} \frac{\mathrm{d}\boldsymbol{x}}{\mathrm{d}t} &= \overline{\boldsymbol{F}}(\boldsymbol{x}). \\ \boldsymbol{x}(0) &= \boldsymbol{x}_0. \end{aligned} \tag{4.5}$$

4.2 Averaging for ODE systems

We will justify the approximation (Equation 4.5) for times up to $\mathcal{O}(1)$ using an averaging method for ODEs (28). For the multiscale system (Equation 4.1) in $(\boldsymbol{x}, \boldsymbol{y})$ let us define the generators

$$\begin{aligned} \mathcal{L}_0 &= \boldsymbol{G}(\boldsymbol{x}, \boldsymbol{y}) \cdot \nabla_y, \\ \mathcal{L}_1 &= \boldsymbol{F}(\boldsymbol{x}, \boldsymbol{y}) \cdot \nabla_x, \end{aligned} \tag{4.6}$$

The backward equation corresponding to (Equation 4.1) is given by

$$\frac{\partial v}{\partial t} = \frac{1}{\varepsilon} \mathcal{L}_0 v + \mathcal{L}_1 v. \tag{4.7}$$

We seek a solution for $v(\boldsymbol{x}, \boldsymbol{y}, t)$ in the form of a perturbation expansion

$$v = v_0 + \varepsilon v_1 + \mathcal{O}(\varepsilon^2) \tag{4.8}$$

Up to the leading two orders we have

$$\mathcal{O}(1/\varepsilon): \quad \mathcal{L}_0 v_0 = 0, \tag{4.9a}$$

$$\mathcal{O}(1): \quad \mathcal{L}_0 v_1 = -\mathcal{L}_1 v_0 + \frac{\partial v_0}{\partial t}. \tag{4.9b}$$

From (Equation 4.9a) and the ergodicity assumption we conclude that v_0 is a function only in $(\boldsymbol{x}, t)$. Furthermore, integrating both sides of (Equation 4.9b) gives us

$$\begin{aligned} \int \left(-\mathcal{L}_1 v_0 + \frac{\partial v_0}{\partial t}\right) \mathrm{d}\mu_x &= \int \mathcal{L}_0 v_1 \, \mathrm{d}\mu_x \\ &= \lim_{t\to 0} \int \frac{e^{\mathcal{L}_0 t} v_1 - v_1}{t} \, \mathrm{d}\mu_x \\ &= 0, \end{aligned} \tag{4.10}$$

due to the invariance of μ_x with respect to $e^{\mathcal{L}_0 t}$. So if $v_0 \in C^1$ we have

$$\begin{aligned} 0 &= \int \left(\frac{\partial v_0}{\partial t}(\boldsymbol{x}, t) - \boldsymbol{F}(\boldsymbol{x}, \boldsymbol{y}) \cdot \nabla_x v_0(\boldsymbol{x}, t)\right) \mathrm{d}\mu_x(\boldsymbol{y}) \\ &= \frac{\partial v_0}{\partial t}(\boldsymbol{x}, t) - \int \left(\boldsymbol{F}(\boldsymbol{x}, \boldsymbol{y}) \, \mathrm{d}\mu_x(\boldsymbol{y})\right) \cdot \nabla_x v_0(\boldsymbol{x}, t) \\ &= \frac{\partial v_0}{\partial t}(\boldsymbol{x}, t) - \overline{\boldsymbol{F}}(\boldsymbol{x}) \cdot \nabla_x v_0(\boldsymbol{x}, t) \end{aligned} \tag{4.11}$$

This is the backward equation for (Equation 4.5), and from this multiple scale analysis we conclude that the averaged system (Equation 4.5) will hold for times up to $\mathcal{O}(1)$.(28; 29)

4.3 Practical implementation of averaged system

A natural source to look for insight in high-dimensional fast dynamics is statistical mechanics. We will use the linear response theory developed in Chapter 2 and results from the

fluctuation-dissipation theorem to approximate the fast system and reduce the multiscale system Equation 4.1 to a lower-dimensional system of slow variables only.

Following the averaging formalism of the previous section, we express the slow solutions of the two-scale system in (Equation 4.1) and the averaged system in (Equation 4.5) in terms of their respective differentiable flows:

$$\boldsymbol{x}(t) = \phi^t(\boldsymbol{x}_0, \boldsymbol{y}_0) \quad \text{for the two-scale system,} \tag{4.12a}$$

$$\boldsymbol{x}_A(t) = \phi_A^t(\boldsymbol{x}_0) \quad \text{for the averaged system.} \tag{4.12b}$$

(In a slight abuse of notation, $\phi^t(\boldsymbol{x}_0, \boldsymbol{y}_0)$ here represents only the slow-variables component of the flow). If $\varepsilon \ll 1$, then for the identical initial conditions $\boldsymbol{x}_0$ and generic choice of $\boldsymbol{y}_0$, the solution $\boldsymbol{x}_A(t)$ of the averaged system in (Equation 4.5) remains near the solution $\boldsymbol{x}(t)$ of the original two-scale system in (Equation 4.1) for $\mathcal{O}(1)$ times. (28; 30; 31)

However, use of the averaged system (Equation 4.5) requires *a priori* knowledge of the invariant distribution μ_x for all values of $\boldsymbol{x}$ in the solution space, which is a highly nontrivial result and in practice requires significant computation to find long-time trajectories of the fast limiting system (Equation 4.3) for a large set of parameters. As a more practical alternative, we use an approximation to $\overline{\boldsymbol{F}}$ that is localized around a single reference state $\boldsymbol{\xi}$. This reference state could be the observed mean state $\overline{\boldsymbol{x}}$ of the multiscale system or another suitable point near which the dynamics is to be approximated. As we will see in the the numerical results of

Chapters 7 and 8, even though this approximation is local it will be useful for approximating the global dynamics.

Given a reference state $\boldsymbol{\xi}$, we have

$$\overline{\boldsymbol{F}}(\boldsymbol{x}) = \int \boldsymbol{F}(\boldsymbol{x},\boldsymbol{y})\,\mathrm{d}\mu_\xi(\boldsymbol{y}) + \left(\int \boldsymbol{F}(\boldsymbol{x},\boldsymbol{y})\,\mathrm{d}\mu_x(\boldsymbol{y}) - \int \boldsymbol{F}(\boldsymbol{x},\boldsymbol{y})\,\mathrm{d}\mu_\xi(\boldsymbol{y})\right). \tag{4.13}$$

We expect the term in parentheses to be small and we will consider two simple approximations to (Equation 4.13). We begin with the zero-order approximation, given by simply ignoring the difference term:

$$\overline{\boldsymbol{F}}_0(\boldsymbol{x}) = \int \boldsymbol{F}(\boldsymbol{x},\boldsymbol{y})\,\mathrm{d}\mu_\xi(\boldsymbol{y}). \tag{4.14}$$

This approximation of the averaging method is simple to derive and requires minimal computation. It has been suggested (32) as part of a numerical approach for a wide variety of two-timescale systems, where the reference state $\boldsymbol{\xi}$ and invariant measure μ_ξ can be periodically updated to prevent $\|\boldsymbol{x}-\boldsymbol{\xi}\|$ from growing too large. However, while easily implemented, this zero-order approximation can fail to capture some of the more complex dynamics of the two-time coupled system, in particular long-time statistics and linear perturbation response as we shall see in Chapters 7 and 8.

In this work we will primarily use a first-order approximation, derived below. (33) If the fast limiting system (Equation 4.3) is structurally stable for $\boldsymbol{x}=\boldsymbol{\xi}$ known to be the case for Axiom A systems,[ref] $\int \boldsymbol{F}(\boldsymbol{x},\boldsymbol{y})\,\mathrm{d}\mu_x(\boldsymbol{y})$ will depend smoothly on $\boldsymbol{x}$. In this case we will be able

to at least approximate the difference term in (Equation 4.13) with a linear term for $\boldsymbol{x}$ near $\boldsymbol{\xi}$. First, we note that

$$\int \boldsymbol{F}(\boldsymbol{x},\boldsymbol{y})\,\mathrm{d}\mu_x(\boldsymbol{y}) = \lim_{t\to\infty}\int \boldsymbol{F}(\boldsymbol{x},\varphi^t_{\boldsymbol{x}}\boldsymbol{y})\,\mathrm{d}\mu_\xi(\boldsymbol{y}), \tag{4.15}$$

namely that when the system is perturbed, solutions will settle on the new invariant manifold of the perturbed system given sufficient time. Then we can write

$$\int \boldsymbol{F}(\boldsymbol{x},\boldsymbol{y})\,\mathrm{d}\mu_x(\boldsymbol{y}) - \int \boldsymbol{F}(\boldsymbol{x},\boldsymbol{y})\,\mathrm{d}\mu_\xi(\boldsymbol{y}) = \lim_{t\to\infty}\int \left(\boldsymbol{F}(\boldsymbol{x},\varphi^t_{\boldsymbol{x}}\boldsymbol{y}) - \boldsymbol{F}(\boldsymbol{x},\varphi^t_{\boldsymbol{\xi}}\boldsymbol{y})\right)\,\mathrm{d}\mu_\xi(\boldsymbol{y}) \tag{4.16}$$

This is exactly the mean response of $\overline{\boldsymbol{F}}_0(\boldsymbol{x})$ at infinite time to a perturbation of the parameter $\boldsymbol{\xi}$ in the fast limiting system, and using results from the previous chapter we can express this term approximately using the linear response and specifically as a function of the statistics of the unperturbed system. In the next section we present a practical implementation of this linear response closure approximation for two types of coupling: a simple linear coupling and a more general nonlinear coupling.

4.4 Reduced model formula for slow variables of two-timescale systems with linear coupling

The first case we consider is a two-timescale system with linear additive coupling between the slow and fast variables:

$$\begin{cases} \dfrac{\mathrm{d}\boldsymbol{x}}{\mathrm{d}t} = \boldsymbol{f}(\boldsymbol{x}) + \boldsymbol{L}_y\boldsymbol{y}, \\ \dfrac{\mathrm{d}\boldsymbol{y}}{\mathrm{d}t} = \boldsymbol{g}(\boldsymbol{y}) + \boldsymbol{L}_x\boldsymbol{x}, \end{cases} \tag{4.17}$$

where $\boldsymbol{f}$ and $\boldsymbol{g}$ are differentiable functions and $\boldsymbol{L}_x$ and $\boldsymbol{L}_y$ are constant matrices. For a sufficiently large timescale separation we can write an averaged system for slow variables alone:

$$\frac{\mathrm{d}\boldsymbol{x}}{\mathrm{d}t} = \boldsymbol{f}(\boldsymbol{x}) + \boldsymbol{L}_y\overline{\boldsymbol{z}}(\boldsymbol{x}), \tag{4.18}$$

The fast limiting system is given by

$$\frac{\mathrm{d}\boldsymbol{z}}{\mathrm{d}t} = \boldsymbol{g}(\boldsymbol{z}) + \boldsymbol{L}_x\boldsymbol{x}, \tag{4.19}$$

with $\boldsymbol{x}$ as a parameter, and with statistical mean state $\overline{\boldsymbol{z}}(\boldsymbol{x}) := \int \boldsymbol{z}\,\mathrm{d}\mu_x(\boldsymbol{z})$. Linearizing this mean state about an arbitrary reference parameter $\boldsymbol{\xi}$, we have

$$\overline{\boldsymbol{z}}(\boldsymbol{x}) \approx \overline{\boldsymbol{z}}_\xi + A \cdot (\boldsymbol{x} - \boldsymbol{\xi}) \tag{4.20}$$

where $\overline{\boldsymbol{z}}_\xi = \overline{\boldsymbol{z}}(\boldsymbol{\xi})$ and where A is some constant matrix to be determined. If we consider the fast limiting system (Equation 4.19) at $\boldsymbol{x} = \boldsymbol{\xi}$ and perturb it by adding the quantity $\boldsymbol{L}_x(\boldsymbol{x} - \boldsymbol{\xi})$ to the right hand side, the linear response of $\overline{\boldsymbol{z}}_\xi$ to this perturbation is given by (Equation 3.18):

$$\delta\overline{\boldsymbol{z}}_\xi(t) = \left[\int_0^t C_\xi(\tau)\,\mathrm{d}\tau\right]\boldsymbol{L}_x(\boldsymbol{x} - \boldsymbol{\xi}), \tag{4.21}$$

where C_ξ is the autocorrelation function (Equation 3.26) for the fast limiting system (Equation 4.19) at $\boldsymbol{x} = \boldsymbol{\xi}$. For a large timescale separation we define the infinite time linear response operator

$$\boldsymbol{\mathcal{C}}_\xi := \int_0^\infty C_\xi(\tau)\,\mathrm{d}\tau, \tag{4.22}$$

so that $A = \boldsymbol{\mathcal{C}}_\xi \boldsymbol{L}_x$ in Equation 4.19, and derive the first-order reduced system

$$\frac{\mathrm{d}\boldsymbol{x}}{\mathrm{d}t} = \boldsymbol{f}(\boldsymbol{x}) + \boldsymbol{L}_y \overline{\boldsymbol{z}}_\xi + \boldsymbol{L}_y \boldsymbol{\mathcal{C}}_\xi \boldsymbol{L}_x (\boldsymbol{x} - \boldsymbol{\xi}). \tag{4.23}$$

Note that for $\boldsymbol{\mathcal{C}}_\xi$ to be finite the autocorrelation function must decay sufficiently fast, which will be the case for strongly mixing and chaotic systems.

4.5 Reduced model formula for two-timescale systems with nonlinear coupling

We now consider two-timescale systems (Equation 4.1) with somewhat more general coupling between slow and fast variables. We cannot handle the most general case so we will place two restrictions on the multiscal system. First, let us assume that $\boldsymbol{F}$ depends at most quadratically on the fast variables $\boldsymbol{y}$, that is, locally near $(\boldsymbol{x}, \boldsymbol{y}')$ the i-th component of $\boldsymbol{F}(\boldsymbol{x}, \boldsymbol{y})$ is given by

$$F_i(\boldsymbol{x}, \boldsymbol{y}) = F_i(\boldsymbol{x}, \boldsymbol{y}') + \sum_j \frac{\partial F_i(\boldsymbol{x}, \boldsymbol{y}')}{\partial y_j}(y_j - y_j') + \frac{1}{2}\sum_{j,k} \frac{\partial^2 F_i(\boldsymbol{x}, \boldsymbol{y}')}{\partial y_j \partial y_k}(y_j - y_j')(y_k - y_k'). \tag{4.24}$$

With respect to the fast limiting system (Equation 4.3), if we take $\boldsymbol{y}' = \overline{\boldsymbol{z}}(\boldsymbol{x})$ and average over $\mu_{\boldsymbol{x}}$ we have

$$\overline{F}_i(\boldsymbol{x}) := \int F_i(\boldsymbol{x}, \boldsymbol{y}) \, \mathrm{d}\mu_x(\boldsymbol{y}) = F_i(\boldsymbol{x}, \overline{\boldsymbol{z}}(\boldsymbol{x})) + \frac{1}{2} \sum_{j,k} \frac{\partial^2 F_i(\boldsymbol{x}, \overline{\boldsymbol{z}}(\boldsymbol{x}))}{\partial y_j \partial y_k} \Sigma_{jk}(\boldsymbol{x}), \tag{4.25}$$

where $\Sigma_{jk}(\boldsymbol{x})$ is the covariance between y_j and y_k in the fast limiting system. Or, more compactly, the averaged system can be written

$$\overline{\boldsymbol{F}}(\boldsymbol{x}) = \boldsymbol{F}(\boldsymbol{x}, \overline{\boldsymbol{z}}(\boldsymbol{x})) + \frac{1}{2} \frac{\partial^2 \boldsymbol{F}}{\partial \boldsymbol{y}^2}(\boldsymbol{x}, \overline{\boldsymbol{z}}(\boldsymbol{x})) : \Sigma(\boldsymbol{x}), \tag{4.26}$$

where : is the Hadamard (component-wise) product with summation. As we can see, the averaged system depends nonlinearly on the mean state $\overline{\boldsymbol{z}}(\boldsymbol{x})$ and linearly on the covariance $\Sigma(\boldsymbol{x})$. We will derive approximations to these functions around a reference state $\boldsymbol{x} = \boldsymbol{\xi}$ using the appropriate linear response formulas.

Second, let us assume the right hand side of the fast system is of the form:

$$\boldsymbol{G}(\boldsymbol{x}, \boldsymbol{y}) = \boldsymbol{g}(\boldsymbol{y}) + \boldsymbol{H}(\boldsymbol{x})\boldsymbol{y} + \boldsymbol{h}(\boldsymbol{x}) \tag{4.27}$$

where $\boldsymbol{g} : \mathbb{R}^{N_y} \to \mathbb{R}^{N_y}$, $\boldsymbol{h} : \mathbb{R}^{N_x} \to \mathbb{R}^{N_y}$ and $\boldsymbol{H} : \mathbb{R}^{N_x} \to \mathbb{R}^{N_y} \times \mathbb{R}^{N_y}$ are arbitrary functions which may be nonlinear. Let $\overline{\boldsymbol{H}}$ and $\overline{\boldsymbol{h}}$ be the mean values of $\boldsymbol{H}(\boldsymbol{x})$ and $\boldsymbol{h}(\boldsymbol{x})$ in the multiscale system, or else some other appropriate reference values, and define $\delta\boldsymbol{H}(\boldsymbol{x}) := \boldsymbol{H}(\boldsymbol{x}) - \overline{\boldsymbol{H}}$ and

$\delta\boldsymbol{h}(\boldsymbol{x}) := \boldsymbol{h}(\boldsymbol{x}) - \overline{\boldsymbol{h}}$ to be the deviations from these values. Consider then the fast limiting system

$$\begin{aligned}\boldsymbol{G}(\boldsymbol{x},\boldsymbol{z}) &= \boldsymbol{g}(\boldsymbol{z}) + (\overline{\boldsymbol{H}} + \delta\boldsymbol{H}(\boldsymbol{x}))\boldsymbol{z} + (\overline{\boldsymbol{h}} + \delta\boldsymbol{h}(\boldsymbol{x})) \\ &= \boldsymbol{g}(\boldsymbol{z}) + \overline{\boldsymbol{H}}\boldsymbol{z} + \overline{\boldsymbol{h}} + \delta\boldsymbol{H}(\boldsymbol{x})\boldsymbol{z} + \delta\boldsymbol{h}(\boldsymbol{x}).\end{aligned} \tag{4.28}$$

Let $\overline{\boldsymbol{z}}_\xi$ and Σ_ξ be the mean and mean-centered covariance for this system in the unperturbed case where $\delta\boldsymbol{H} = \delta\boldsymbol{h} = 0$. To find a closed formula for (Equation 4.25), we will derive the infinite-time responses of $\overline{\boldsymbol{z}}_\xi$ and Σ_ξ when the forcing terms $\delta\boldsymbol{H}$ and $\delta\boldsymbol{h}$ are nonzero. This will yield the following expressions (see Appendix A for details):

$$\begin{aligned}\overline{\boldsymbol{z}}(\boldsymbol{x}) &= \overline{\boldsymbol{z}}_\xi + \boldsymbol{R}^{L\to\overline{z}} : \delta\boldsymbol{H}(\boldsymbol{x}) + \boldsymbol{R}^{c\to\overline{z}} \left(\delta\boldsymbol{h}(\boldsymbol{x}) + \delta\boldsymbol{H}(\boldsymbol{x})\overline{\boldsymbol{z}}_\xi\right) \\ \Sigma(\boldsymbol{x}) &= \Sigma_\xi + \boldsymbol{R}^{L\to\Sigma} : \delta\boldsymbol{H}(\boldsymbol{x}) + \boldsymbol{R}^{c\to\Sigma} \left(\delta\boldsymbol{h}(\boldsymbol{x}) + \delta\boldsymbol{H}(\boldsymbol{x})\overline{\boldsymbol{z}}_\xi\right),\end{aligned} \tag{4.29}$$

where : denotes the Frobenius (component-wise) inner product, and where the components of these four linear response operators at $t = \infty$ are given by

$$\begin{aligned}
R_{ij}^{c\to\overline{z}} &= \int_0^\infty \left[\lim_{S\to\infty} \frac{1}{S}\int_0^S (z_i(s+\tau) - \overline{z}_i)(z_k(s) - \overline{z}_k)\,\mathrm{d}s\right] \mathrm{d}\tau\ (\Sigma_\xi^{-1})_{kj} \\
R_{ijk}^{L\to\overline{z}} &= \int_0^\infty \left[\lim_{S\to\infty} \frac{1}{S}\int_0^S (z_i(s+\tau) - \overline{z}_i)(z_l(s) - \overline{z}_l)(z_k(s) - \overline{z}_k)\,\mathrm{d}s\right] \mathrm{d}\tau\ (\Sigma_\xi^{-1})_{lj} \\
R_{ijk}^{c\to\Sigma} &= \int_0^\infty \left[\lim_{S\to\infty} \frac{1}{S}\int_0^S (z_i(s+\tau) - \overline{z}_i)(z_j(s+\tau) - \overline{z}_j)(z_l(s) - \overline{z}_l)\,\mathrm{d}s\right] \mathrm{d}\tau\ (\Sigma_\xi^{-1})_{lk} \\
R_{ijkl}^{L\to\Sigma} &= \int_0^\infty \Bigg[\lim_{S\to\infty} \frac{1}{S}\int_0^S (z_i(s+\tau) - \overline{z}_i)(z_j(s+\tau) - \overline{z}_j) \times \\
&\qquad \times (z_m(s) - \overline{z}_m)(z_l(s) - \overline{z}_l)\,\mathrm{d}s\ (\Sigma_\xi^{-1})_{mk} - (\Sigma_\xi)_{ij}\delta_{kl}\Bigg] \mathrm{d}\tau,
\end{aligned} \tag{4.30}$$

where $\overline{z}_i$ is the i-th component of $\overline{\boldsymbol{z}}_\xi$ and δ_{kl} is the Kronecker delta. So, using (Equation 4.29) and (Equation 4.25) we have a closure approximation for the evolution of the slow variables, in practice requiring only a computed trajectory of the fast limiting system (Equation 4.28) that is sufficiently long to estimate its mean and covariance matrix.

CHAPTER 5

CRITERIA FOR SIMILARITY OF PERTURBATION RESPONSE BETWEEN THE TWO-SCALE SYSTEM AND ITS AVERAGED SLOW SYSTEM

We turn our attention now to the similarity of the averaged model to its underlying multi-scale model. In this chapter we attempt to establish criteria for the similarity of the responses of these systems to equivalent perturbations. [1]

Consider the two-scale system in (Equation 4.1) and the averaged system in (Equation 4.5), each perturbed at the slow variables by a small time-dependent forcing $\boldsymbol{\delta f}(t)$ starting at $t = 0$:

$$\begin{cases} \dfrac{\mathrm{d}\boldsymbol{x}}{\mathrm{d}t} = \boldsymbol{F}(\boldsymbol{x}, \boldsymbol{y}) + \boldsymbol{\delta f}(t), \\ \dfrac{\mathrm{d}\boldsymbol{y}}{\mathrm{d}t} = \dfrac{1}{\varepsilon}\boldsymbol{G}(\boldsymbol{x}, \boldsymbol{y}), \end{cases} \tag{5.1a}$$

$$\frac{\mathrm{d}\boldsymbol{x}}{\mathrm{d}t} = \overline{\boldsymbol{F}}(\boldsymbol{x}) + \boldsymbol{\delta f}(t), \tag{5.1b}$$

where

$$\overline{\boldsymbol{F}}(\boldsymbol{x}) = \int \boldsymbol{F}(\boldsymbol{x}, \boldsymbol{y}) \, \mathrm{d}\mu_x(\boldsymbol{y}). \tag{5.2}$$

---

[1] Material in this chapter has been submitted for publication and is awaiting review.(34)

We can express the slow variable trajectories of these perturbed systems in terms of differentiable flows:

$$\hat{\boldsymbol{x}}(t) = \hat{\phi}^t(\boldsymbol{x}_0, \boldsymbol{y}_0), \tag{5.3a}$$

$$\hat{\boldsymbol{x}}_A(t) = \hat{\phi}_A^t(\boldsymbol{x}_0). \tag{5.3b}$$

Suppose μ and μ_A are ergodic invariant probability measures for the unperturbed two-scale system (Equation 4.1) and averaged system (Equation 4.5), respectively. Let $b(\boldsymbol{x})$ be a differentiable observable function of the slow variables with well-defined averages

$$\langle b \rangle := \int b(\boldsymbol{x}) \, \mathrm{d}\mu(\boldsymbol{x}, \boldsymbol{y}), \tag{5.4a}$$

$$\langle b \rangle_A := \int b(\boldsymbol{x}) \, \mathrm{d}\mu_A(\boldsymbol{x}). \tag{5.4b}$$

The average responses of these quantities, denoted by $\delta\langle b \rangle(t)$ and $\delta\langle b \rangle_A(t)$ for the respective systems, are defined as

$$\delta\langle b \rangle(t) = \int \left(b(\hat{\phi}^t(\boldsymbol{x}, \boldsymbol{y})) - b(\phi^t(\boldsymbol{x}, \boldsymbol{y})) \right) \mathrm{d}\mu(\boldsymbol{x}, \boldsymbol{y}), \tag{5.5a}$$

$$\delta\langle b \rangle_A(t) = \int \left(b(\hat{\phi}_A^t(\boldsymbol{x})) - b(\phi_A^t \boldsymbol{x}) \right) \mathrm{d}\mu_A(\boldsymbol{x}), \tag{5.5b}$$

For $\boldsymbol{\delta f}$ sufficiently small we expect these responses to be approximately linear and we will approximate them by the following linear response relations, as in (Equation 3.18):

$$\delta\langle b\rangle(t) \approx \int_0^t \boldsymbol{R}(t-s)\boldsymbol{\delta f}(s)\,\mathrm{d}s, \qquad \boldsymbol{R}(t) = \int \nabla_x \left(b(\phi^t(\boldsymbol{x},\boldsymbol{y}))\right)\,\mathrm{d}\mu(\boldsymbol{x},\boldsymbol{y}), \tag{5.6a}$$

$$\delta\langle b\rangle_A(t) \approx \int_0^t \boldsymbol{R}_A(t-s)\boldsymbol{\delta f}(s)\,\mathrm{d}s, \qquad \boldsymbol{R}_A(t) = \int \nabla_x \left(b(\phi_A^t(\boldsymbol{x}))\right)\,\mathrm{d}\mu_A(\boldsymbol{x}). \tag{5.6b}$$

Here it is apparent that any differences between $\delta\langle b\rangle(t)$ and $\delta\langle b\rangle_A(t)$ are due to differences between $\boldsymbol{R}(t)$ and $\boldsymbol{R}_A(t)$, since $\boldsymbol{\delta f}$ is identical in both cases. The differences between $\boldsymbol{R}(t)$ and $\boldsymbol{R}_A(t)$ are, in turn, caused by the differences between the flows ϕ^t and ϕ_A^t and between the invariant distribution measures μ and μ_A, which are difficult to quantify in practice. In what follows we express the differences between $\boldsymbol{R}(t)$ and $\boldsymbol{R}_A(t)$ via statistically tractable quantities. First, we make the assumption that the invariant measures μ and μ_A are absolutely continuous with respect to the Lebesgue measure with distribution densities $\rho(\boldsymbol{x},\boldsymbol{y})$ and $\rho_A(\boldsymbol{x})$, respectively, so that we have:

$$\boldsymbol{R}(t) = \int \nabla_x \left(b(\phi^t(\boldsymbol{x},\boldsymbol{y}))\right)\rho(\boldsymbol{x},\boldsymbol{y})\,\mathrm{d}\boldsymbol{x}\,\mathrm{d}\boldsymbol{y}, \tag{5.7a}$$

$$\boldsymbol{R}_A(t) = \int \nabla_x \left(b(\phi_A^t(\boldsymbol{x}))\right)\rho_A(\boldsymbol{x})\,\mathrm{d}\boldsymbol{x}. \tag{5.7b}$$

Integration by parts yields

$$\boldsymbol{R}(t) = -\int b(\phi^t(\boldsymbol{x},\boldsymbol{y}))\nabla_x\rho(\boldsymbol{x},\boldsymbol{y})\,\mathrm{d}\boldsymbol{x}\,\mathrm{d}\boldsymbol{y}, \tag{5.8a}$$

$$\boldsymbol{R}_A(t) = -\int b(\phi_A^t(\boldsymbol{x}))\nabla\rho_A(\boldsymbol{x})\,\mathrm{d}\boldsymbol{x}. \tag{5.8b}$$

Let us express the multiscale distribution density $\rho(\boldsymbol{x},\boldsymbol{y})$ as the product of its marginal distribution $\bar{\rho}(\boldsymbol{x})$ and conditional distribution $\rho(\boldsymbol{y}|\boldsymbol{x})$, given respectively by

$$\bar{\rho}(\boldsymbol{x}) = \int \rho(\boldsymbol{x},\boldsymbol{y})\,\mathrm{d}\boldsymbol{y}, \tag{5.9}$$

and

$$\rho(\boldsymbol{y}|\boldsymbol{x}) = \frac{\rho(\boldsymbol{x},\boldsymbol{y})}{\bar{\rho}(\boldsymbol{x})}. \tag{5.10}$$

Now the formula for the linear response operator $\boldsymbol{R}(t)$ above can be written as

$$\boldsymbol{R}(t) = -\int b(\phi^t(\boldsymbol{x},\boldsymbol{y}))\rho(\boldsymbol{y}|\boldsymbol{x})\frac{\partial\bar{\rho}(\boldsymbol{x})}{\partial\boldsymbol{x}}\,\mathrm{d}\boldsymbol{y}\,\mathrm{d}\boldsymbol{x} - \int b(\phi^t(\boldsymbol{x},\boldsymbol{y}))\frac{\partial\rho(\boldsymbol{y}|\boldsymbol{x})}{\partial\boldsymbol{x}}\bar{\rho}(\boldsymbol{x})\,\mathrm{d}\boldsymbol{y}\,\mathrm{d}\boldsymbol{x}. \tag{5.11}$$

Since we expect $\phi^t(\boldsymbol{x},\boldsymbol{y})$ and $\phi_A^t(\boldsymbol{x})$ to be close for small t, we can take a first-order Taylor expansion for b in a neighborhood of $\phi_A^t(\boldsymbol{x})$:

$$b(\phi^t(\boldsymbol{x},\boldsymbol{y})) \approx b(\phi_A^t(\boldsymbol{x})) + \nabla b\left(\phi_A^t(\boldsymbol{x})\right)^T\left(\phi^t(\boldsymbol{x},\boldsymbol{y}) - \phi_A^t(\boldsymbol{x})\right) \tag{5.12}$$

the second integral in the right-hand side of (Equation 5.11) becomes

$$\begin{aligned}-\int b(\phi^t(\boldsymbol{x},\boldsymbol{y}))\frac{\partial\rho(\boldsymbol{y}|\boldsymbol{x})}{\partial\boldsymbol{x}}\bar{\rho}(\boldsymbol{x})\,\mathrm{d}\boldsymbol{y}\,\mathrm{d}\boldsymbol{x} = -\int b(\phi_A^t(\boldsymbol{x}))\left(\int\frac{\partial\rho(\boldsymbol{y}|\boldsymbol{x})}{\partial\boldsymbol{x}}\,\mathrm{d}\boldsymbol{y}\right)\bar{\rho}(\boldsymbol{x})\,\mathrm{d}\boldsymbol{x} - \\ -\int\nabla b\left(\phi_A^t(\boldsymbol{x})\right)^T\left(\phi^t(\boldsymbol{x},\boldsymbol{y}) - \phi_A^t(\boldsymbol{x})\right)\frac{\partial\rho(\boldsymbol{y}|\boldsymbol{x})}{\partial\boldsymbol{x}}\bar{\rho}(\boldsymbol{x})\,\mathrm{d}\boldsymbol{y}\,\mathrm{d}\boldsymbol{x}.\end{aligned} \tag{5.13}$$

The first integral in the right-hand side of (Equation 5.13) is zero due to the identity

$$\int \rho(\boldsymbol{y}|\boldsymbol{x})\,\mathrm{d}\boldsymbol{y} = 1 \quad \text{for all } \boldsymbol{x}, \tag{5.14}$$

so we have

$$\begin{aligned} -\int b(\phi^t(\boldsymbol{x},\boldsymbol{y}))^T \frac{\partial \rho(\boldsymbol{y}|\boldsymbol{x})}{\partial \boldsymbol{x}} \bar{\rho}(\boldsymbol{x})\,\mathrm{d}\boldsymbol{y}\,\mathrm{d}\boldsymbol{x} &= -\int \nabla b(\phi_A^t(\boldsymbol{x}))^T \left(\phi^t(\boldsymbol{x},\boldsymbol{y}) - \phi_A^t(\boldsymbol{x})\right) \frac{\partial \rho(\boldsymbol{y}|\boldsymbol{x})}{\partial \boldsymbol{x}} \bar{\rho}(\boldsymbol{x})\,\mathrm{d}\boldsymbol{y}\,\mathrm{d}\boldsymbol{x} \\ &= O(\|\phi^t(\boldsymbol{x},\boldsymbol{y}) - \phi_A^t(\boldsymbol{x})\|). \end{aligned} \tag{5.15}$$

The quantity $\phi^t(\boldsymbol{x},\boldsymbol{y}) - \phi_A^t(\boldsymbol{x})$ will be small compared with either $\phi^t(\boldsymbol{x},\boldsymbol{y})$ or $\phi_A^t(\boldsymbol{x})$ for relevant values of t. Neglecting this term in (Equation 5.8), we have

$$\boldsymbol{R}(t) = -\int b(\phi^t(\boldsymbol{x},\boldsymbol{y}))\rho(\boldsymbol{y}|\boldsymbol{x})\nabla\bar{\rho}(\boldsymbol{x})\,\mathrm{d}\boldsymbol{y}\,\mathrm{d}\boldsymbol{x}, \tag{5.16a}$$

$$\boldsymbol{R}_A(t) = -\int b(\phi_A^t(\boldsymbol{x}))\nabla\rho_A(\boldsymbol{x})\,\mathrm{d}\boldsymbol{x}. \tag{5.16b}$$

We now express $\bar{\rho}(\boldsymbol{x})$ and $\rho_A(\boldsymbol{x})$ as exponentials

$$\bar{\rho}(\boldsymbol{x}) = e^{-\bar{q}(\boldsymbol{x})}, \qquad \rho_A(\boldsymbol{x}) = e^{-q_A(\boldsymbol{x})}, \tag{5.17}$$

where $\bar{q}(\boldsymbol{x})$ and $q_A(\boldsymbol{x})$ are smooth functions that grow to infinity as $\boldsymbol{x}$ becomes infinite. This gives us

$$\begin{aligned}\boldsymbol{R}(t) &= \int b(\phi^t(\boldsymbol{x},\boldsymbol{y}))\nabla\bar{q}(\boldsymbol{x})\rho(\boldsymbol{y}|\boldsymbol{x})\bar{\rho}(\boldsymbol{x})\,\mathrm{d}\boldsymbol{y}\,\mathrm{d}\boldsymbol{x} \\ &= \int b(\phi^t(\boldsymbol{x},\boldsymbol{y}))\nabla\bar{q}(\boldsymbol{x})\,\mathrm{d}\mu(\boldsymbol{x},\boldsymbol{y}),\end{aligned} \tag{5.18a}$$

$$\begin{aligned}\boldsymbol{R}_A(t) &= \int b(\phi_A^t(\boldsymbol{x}))\nabla q_A(\boldsymbol{x})\rho_A(\boldsymbol{x})\,\mathrm{d}\boldsymbol{x} \\ &= \int b(\phi_A^t(\boldsymbol{x}))\nabla q_A(\boldsymbol{x})\mu_A(\boldsymbol{x}).\end{aligned} \tag{5.18b}$$

By the ergodicity assumption we can replace invariant measure averages with long-term time averages to arrive at the following time correlation functions:

$$\boldsymbol{R}(t) = \lim_{S\to\infty}\frac{1}{S}\int_0^S b(\boldsymbol{x}(s+t))\nabla\bar{q}(\boldsymbol{x}(s))\,\mathrm{d}s, \tag{5.19a}$$

$$\boldsymbol{R}_A(t) = \lim_{S\to\infty}\frac{1}{S}\int_0^S b(\boldsymbol{x}_A(s+t))\nabla q_A(\boldsymbol{x}_A(s))\,\mathrm{d}s. \tag{5.19b}$$

Since b is arbitrary, we can conclude that for $\boldsymbol{R}_A(t)$ to approximate $\boldsymbol{R}(t)$ for finite times, we need the following three conditions to be approximately satisfied:

1. For equivalent initial conditions, $\boldsymbol{x}_A(t)$ should approximate $\boldsymbol{x}(t)$, that is $\phi^t(\boldsymbol{x},\boldsymbol{y}) - \phi_A^t(\boldsymbol{x})$ should indeed be small, on the finite time scale of decay of the correlation functions in (Equation 5.19);

2. The invariant distribution $\rho_A(\boldsymbol{x})$ of the averaged system in (Equation 4.5) should be similar to the $\boldsymbol{x}$-marginal $\bar{\rho}(\boldsymbol{x})$ of the invariant distribution of the two-scale dynamical system (Equation 4.1);

3. The time autocorrelation functions of the averaged system in (Equation 4.5) should be similar to those of the slow variables of the two-scale system in (Equation 4.1).

The first condition is expected to hold for relevant values of t based on the scale analysis for the averaged dynamics in Chapter 4 and (28; 29). In the following chapter we present a nonlinear two-timescale toy model, and we will verify the second and third conditions numerically for this system in Chapter 7. In Chapter 8 we will validate the above results for the similarity of perturbation response between this model and its corresponding approximate average systems in several parameter regimes.

CHAPTER 6

TESTBED – THE LORENZ 96 SYSTEM

The methods in the previous chapters hold for systems satisfying a number of hypotheses: they should be ergodic with hyperbolic structure on an invariant manifold and mixing on an appropriate timescale. In a realistic or useful model described by a high-dimensional nonlinear system, we may have experimental evidence of a chaotic or Anosov flow but no rigorous proof that these hypotheses are satisfied. Furthermore, the averaging theory holds formally in the limit $\varepsilon \to 0$ and only guarantees that solutions will stay close for times $\mathcal{O}(1)$, but typically we will have $\varepsilon > 0$ and we may be interested in more general properties of a system such as long-time statistics or sensitivity to perturbation.

In this chapter we describe a high-dimensional nonlinear two-timescale system to which we apply the averaging methodology of Chapter 4. By construction, this toy model is relatively simple to analyze yet has a number of properties which make it relevant to real-world geophysical applications. In the appropriate parameter regimes, this system has the necessary properties of mixing, etc., to justify the derivation of an averaged reduced model and the statistical analyses. In Chapters 7 and 8 we will present experimental evidence that the reduced models are indeed useful as approximations to the multiscale system even as the conditions are relaxed.

6.1 A simple system to study predictability

In an exposition on predictability in models of planetary atmosphere (35), Edward Lorenz proposed the system

$$\dot{x}_i = x_{i-1}(x_{i+1} - x_{i-2}) - x_i + F, \qquad i = 1, \ldots, N, \tag{6.1}$$

with periodic boundary condition $x_{i+N} = x_i$. This system has generic features of geophysical flows, namely a nonlinear advection-like term which conserves quadratic energy as well as linear viscous damping and constant forcing terms. For many parameter regimes this system exhibits linearly unstable waves, mixing, and chaos (15), all of which are present in earth's atmosphere. Its simple formulation, with invariance under index translation and a constant forcing parameter F, allows for straightforward analysis - in particular the long-time statistics of each variable is identical and is controlled by F. Additionally, the chaos and mixing of the system increase with the forcing parameter, with decaying solutions for F near zero, periodic and traveling wave solutions for F slightly larger than zero, weakly chaotic solutions around $F = 5$, and increasing chaos and mixing for higher F.

Thorough analysis of this system and its statistical properties can be found in other works such as (15).

6.2 The two-scale Lorenz 96 system

If we recall, the primary rate at which an infinitesimal error increases or diminishes in a system is dictated by the leading Lyapunov exponent λ_1. For a system which is chaotic, believed

to be the case for earth's atmosphere, we have $\lambda_1 > 0$, and there is a corresponding notion of the *doubling time* of errors given by $t = \frac{\ln 2}{\lambda_1}$. Lorenz noted that doubling times for contemporary atmospheric models were estimated at 1.5 days, yet a convective system can realistically double in intensity in under an hour. Models calibrated to resolve synoptic and mesoscale phenomena would generally not be able to resolve the relatively small convective cells, restricted by their discretization, so these models might underrepresent error propagation. To study predictability for such systems with rapidly evolving subgrid-scale phenomena, Lorenz proposed a two-time system given by

$$\begin{cases} \dot{x}_i = x_{i-1}(x_{i+1} - x_{i-2}) - x_i + F_x - \dfrac{\lambda_y}{J}\displaystyle\sum_{j=1}^{J} y_{i,j}, \\ \dot{y}_{i,j} = \dfrac{1}{\varepsilon}\left[y_{i,j+1}(y_{i,j-1} - y_{i,j+2}) - y_{i,j} + F_y + \lambda_x x_i\right], \end{cases} \tag{6.2}$$

referred to as the Lorenz 96 system, where $1 \leq i \leq N_x, 1 \leq j \leq J$, with periodic boundary conditions $x_{i+N_x} = x_i$, $y_{i+N_x,j} = y_{i,j}$ and $y_{i,j+J} = y_{i+1,j}$. Here F_x and F_y are constant forcing terms, λ_x and λ_y constant coupling parameters, and ε is the explicit time scale separation parameter. It is easy to verify that the nonlinear and coupling terms conserve energy of the form

$$E = \frac{\lambda_x}{2}\sum_{i=1}^{N_x} x_i^2 + \frac{\varepsilon\lambda_y}{2J}\sum_{i=1}^{N_x}\sum_{j=1}^{J} y_{i,j}^2. \tag{6.3}$$

In Lorenz's original formulation of the two-scale system he used $F_x \equiv F_y \equiv 0$, so that the local intensity of one system drives the local intensity of the other, but we take them to be nonzero to explore a variety of dynamical regimes.

6.3 Rescaling the Lorenz 96 system

To simplify the analysis of coupling trends for the two-time system, we perform a change of variables to scale out the dependence of the mean state and mean energy on the forcing term F. Given the long-term mean $\overline{x}$ and standard deviation σ for the uncoupled system (Equation 6.1), we rescale $\boldsymbol{x}$ and t as

$$x_i = \overline{x} + \sigma \hat{x}_i, \quad t = \frac{\tau}{\sigma}, \tag{6.4}$$

where the normalized variables $\hat{\boldsymbol{x}}$ have zero mean and unit standard deviation, while their time autocorrelation functions have normalized scaling across different dynamical regimes (that is, different forcings F) for short correlation times τ. In the rescaled variables, the uncoupled Lorenz model becomes

$$\dot{\hat{x}}_i = \left(\hat{x}_{i-1} + \frac{\overline{x}}{\sigma}\right)(\hat{x}_{i+1} - \hat{x}_{i-2}) - \frac{\hat{x}_i}{\sigma} + \frac{F - \overline{x}}{\sigma^2}, \tag{6.5}$$

where $\overline{x}$ and σ are functions of F, determined by sampling along a long trajectory of (Equation 6.1). This rescaling was previously used in (36; 33; 37), and a slightly different normalization was analyzed extensively in (15).

We similarly rescale the coupled two-scale Lorenz 96 model. Dropping the "hat" we have:

$$\begin{cases} \dfrac{\mathrm{d}x_i}{\mathrm{d}t} = \left(x_{i-1} + \dfrac{\overline{x}}{\sigma_x}\right)(x_{i+1} - x_{i-2}) - \dfrac{x_i}{\sigma_x} + \dfrac{F_x - \overline{x}}{{\sigma_x}^2} - \dfrac{\lambda_y}{J}\displaystyle\sum_{j=1}^{J} y_{i,j}, \\ \varepsilon \dfrac{\mathrm{d}y_{i,j}}{\mathrm{d}t} = \left(y_{i,j+1} + \dfrac{\overline{y}}{\sigma_y}\right)(y_{i,j-1} - y_{i,j+2}) - \dfrac{y_{i,j}}{\sigma_y} + \dfrac{F_y - \overline{y}}{{\sigma_y}^2} + \lambda_x x_i, \end{cases} \tag{6.6}$$

where $\{\overline{x},\ \sigma_x\}$ and $\{\overline{y},\ \sigma_y\}$ are the long term means and standard deviations of the uncoupled systems with F_x or F_y as constant forcing, respectively. We will focus on this rescaled coupled Lorenz 96 system for the closure approximation. The normalization allows us to control the qualitative dynamics of both slow and fast systems using the forcing parameters F_x and F_y, respectively, without significantly changing the mean state of the coupled system; the necessary tradeoff being that the normalizing constants must be found via statistical sampling for each parameter regime under consideration. For further information on the rescaled Lorenz 96 system, including a discussion of how the slow dynamics are affected by the coupled fast dynamics, see (36).

6.4 Reduced models for the rescaled Lorenz 96 system

For a reference state $\boldsymbol{\xi}$ the fast limiting system for the rescaled Lorenz 96 is given by

$$\dot{y}_{i,j} = \left(y_{i,j+1} + \frac{\overline{y}}{\sigma_y}\right)(y_{i,j-1} - y_{i,j+2}) - \frac{y_{i,j}}{\sigma_y} + \frac{F_y - \overline{y}}{{\sigma_y}^2} + \lambda_x \xi_i, \tag{6.7}$$

the zero-order reduced system is given by

$$\dot{\hat{x}}_i = \left(\hat{x}_{i-1} + \frac{\overline{x}}{\sigma_x}\right)(\hat{x}_{i+1} - \hat{x}_{i-2}) - \frac{\hat{x}_i}{\sigma_x} + \frac{F_x - \overline{x}}{\sigma_x^2} - \lambda_y \overline{\boldsymbol{z}}_\xi. \tag{6.8}$$

and the first-order reduced system is given by

$$\dot{\hat{x}}_i = \left(\hat{x}_{i-1} + \frac{\overline{x}}{\sigma_x}\right)(\hat{x}_{i+1} - \hat{x}_{i-2}) - \frac{\hat{x}_i}{\sigma_x} + \frac{F_x - \overline{x}}{\sigma_x^2} - \lambda_y \overline{\boldsymbol{z}}_\xi + \left(L_y \boldsymbol{\mathcal{C}}_\xi L_x(\boldsymbol{x} - \boldsymbol{\xi})\right)_i, \tag{6.9}$$

where L_y and L_x are the linear coupling matrices of (Equation 6.6) and $\boldsymbol{\mathcal{C}}_\xi$ is the infinite time linear response operator (Equation 4.22) for the fast limiting system (Equation 6.7).

Before any numerical tests are performed, we can anticipate that the zero-order reduced system (Equation 6.8) may be inadequate for this model even for simple linear coupling. Once the reference state $\boldsymbol{\xi}$ is determined and mean of the fast limiting system $\overline{\boldsymbol{z}}_\xi$ is computed, we expect the perturbation term $\lambda_y \overline{\boldsymbol{z}}_\xi$ to be small, since the uncoupled systems have zero mean in the uncoupled setting. As a result we expect this to have only a small effect on the uncoupled slow dynamics. However, it has been shown that coupling a fast chaotic system to a slow chaotic system has a suppressive effect on the chaos of the slow system (36), and apparently this phenomenon will not be manifest in the zero-order model.

6.5 Lorenz 96 system with higher order coupling

In addition to the linearly coupled test model presented above, we also consider a Lorenz 96 system with higher order mixed coupling terms. With a similar rescaling as above, we have

$$\begin{cases} \dfrac{\mathrm{d}x_i}{\mathrm{d}t} = \left(x_{i-1} + \dfrac{\overline{x}}{\sigma_x}\right)(x_{i+1} - x_{i-2}) - \dfrac{x_i}{\sigma_x} + \dfrac{F_x - \overline{x}}{{\sigma_x}^2} - \\ \qquad\qquad - \dfrac{\lambda_y}{J}\displaystyle\sum_{j=1}^{J}\left[(a + bx_i)y_{i,j} + (c + dx_i)(y_{i,j}^2 - 1)\right], \\ \varepsilon\dfrac{\mathrm{d}y_{i,j}}{\mathrm{d}t} = \left(y_{i,j+1} + \dfrac{\overline{y}}{\sigma_y}\right)(y_{i,j-1} - y_{i,j+2}) - \dfrac{y_{i,j}}{\sigma_y} + \dfrac{F_y - \overline{y}}{{\sigma_y}^2} + \\ \qquad\qquad + \lambda_x\left[(a + cy_{i,j})x_i + (b + dy_{i,j})(x_i^2 - 1)\right], \end{cases} \tag{6.10}$$

as proposed in (37), where the coupling term also conserves the quadratic energy functional (Equation 6.3). We see that $\boldsymbol{h}(\boldsymbol{x})$ and $\boldsymbol{H}(\boldsymbol{x})$ in (Equation 4.27) are given by

$$\begin{aligned} h_{i,j}(\boldsymbol{x}) &= \frac{\lambda_x}{\varepsilon}(ax_i + bx_i^2) \\ H_{(i,j),(i',j')}(\boldsymbol{x}) &= \frac{\lambda_x}{\varepsilon} delta_{(i,j),(i',j')}(cx_i + dx_i^2). \end{aligned} \tag{6.11}$$

We also have

$$\frac{1}{2}\frac{\partial^2 F_i}{\partial \boldsymbol{y}^2}(\boldsymbol{x}) : \Sigma(\boldsymbol{x}) = -\frac{\lambda_y}{J}(c + dx_i)\sum_{j=1}^{J} \Sigma_{(i,j),(i',j')}(\boldsymbol{x}). \tag{6.12}$$

In particular, since only the diagonal entries of the covariance matrix $\Sigma(\boldsymbol{x})$ are needed and since $\boldsymbol{H}(\boldsymbol{x})$ is a diagonal matrix, the infinite-time linear response operators $\boldsymbol{R}^{L\to\overline{z}}, \boldsymbol{R}^{c\to\overline{z}}, \boldsymbol{R}^{L\to\Sigma}$, and $\boldsymbol{R}^{c\to\Sigma}$ used in the reduced model (as described in Section 4.5) are 2-dimensional matrices and not 3- and 4-dimensional tensors.

CHAPTER 7

COMPARISON OF STATISTICAL PROPERTIES OF REDUCED MODELS

In this chapter we describe the results of a numerical study of the rescaled Lorenz 96 system (Equation 6.6) and its corresponding reduced models of slow dynamics. In particular we investigate the ability of the reduced systems to capture the statistical properties of long-time solutions in the slow variables as well their mean response to external perturbations. [1]

We consider several parameter regimes, varying the degrees of forcing, coupling, and timescale separation. Held constant will be the size of the systems, with a slow system of twenty variables ($N_x = 20$) coupled to a fast system of eighty variables ($N_y = 80$). For numerical integration of these ODES we use a fourth order explicit Runge-Kutta method with timestep $dt = \varepsilon/10$ in the multiscale system and $dt = 1/10$ in the reduced system.

In Chapter 5 we outlined the main requirements for a reduced model to accurately capture the response of the corresponding two-scale system: the approximation of joint distribution density functions (DDF) for the slow variables, and the time autocorrelation functions of the time series. It is, of course, not computationally feasible to directly compare the 20-dimensional DDFs and autocorrelations for all possible test functions. However, it is possible to compare the univariate marginal DDFs and autocorrelations for an individual slow variable, and thus have

---

[1] Material in this chapter has been submitted for publication and is awaiting review.(34)

a rough estimate on how the statistical properties of the multiscale dynamics are reproduced by the reduced model.

Note on the choice of parameter regimes: the forcing F_y must be large enough so the fast limiting system is in a chaotic regime with sufficiently fast decay of the autocorrelation function; we focus in particular on the strongly mixing regime $F_y = 12$. The coupling strength λ_x and λ_y will be positive, but not larger than 1; we will see that as these parameters increase the full system will be more difficult to approximate with averaged systems.

7.1 Statistical comparison for L96 with linear coupling

In Figure 1 we compare the distribution density functions and autocorrelation functions of the slow variables. The DDFs are computed using bin-counting, and the autocorrelation function $\langle x_i(t)x_i(t+s)\rangle$, averaged over t, is normalized by the variance $\langle x_i^2\rangle$. Results from three parameter regimes are presented. In all three regimes the fast system is chaotic and weakly mixing ($F_y = 12$) and the coupling strength $\lambda_x = \lambda_y = 0.4$ is chosen to be large enough so that the multiscale dynamics are challenging to approximate - in particular they are poorly approximated by a zero-order system (as we shall see in Figure 2, see also (33)). Of particular interest are timescale separations of $\varepsilon = 10^{-1}$ and $\varepsilon = 10^{-2}$.

First we consider a slow regime which is chaotic and strongly mixing ($F_x = 16$) with timescale separation $\varepsilon = 10^{-1}$. Due to the rapid strong mixing of this parameter regime, the large scale behavior is quite similar for a larger timescale separation. Figures are presented for the timescale separation $\varepsilon = 10^{-1}$ only, because in this regime the situation is very similar for $\varepsilon = 10^{-2}$. We also consider a slow regime which is weakly chaotic and quasi-periodic ($F_x = 8$).

In this regime the coupled dynamics are more sensitive to the timescale separation so we present results for both $\varepsilon = 10^{-1}$ and $\varepsilon = 10^{-2}$. Similar plots of statistical quantities for other regimes, including regimes with less chaotic behavior, can be found in (33).

In order to systematically compare DDFs for many parameter regimes, we introduce two metrics on the space of distributions. First is the Jensen-Shannon metric (38) which and is given by

$$m_{\mathrm{JS}}(P,Q) = \frac{1}{\sqrt{2}}\left(\int_{-\infty}^{\infty} \log\left(\frac{2p(x)}{p(x)+q(x)}\right) p(x)dx + \int_{-\infty}^{\infty} \log\left(\frac{2q(x)}{p(x)+q(x)}\right) q(x)dx\right)^{1/2}, \tag{7.1}$$

where p and q are densities on distributions P and Q. This metric, derived from the information-theoretic Kullback-Leibler divergence (39), is a symmetric quantity related to the relative entropy of the two distributions and provides a sense of the amount of information lost by using one distribution in place of the other. The second metric we consider is the earth mover's distance, also known as the first Wasserstein metric, commonly used in image classification and originally motivated by transportation theory (40). By analogy, this metric represents the minimum work needed to move one distribution function to another as though they were piles of dirt; the energy cost is the amount of 'dirt' times the Euclidean ground distance it moved. For distribution functions of one-dimensional random variables, the earth mover's distance is the L^1 norm of the difference of the cumulative distributions:

$$m_{\mathrm{EM}}(P,Q) = \int_{-\infty}^{\infty} \left| \int_{-\infty}^{x} (p(s) - q(s))\, \mathrm{d}s \right| \mathrm{d}x. \tag{7.2}$$

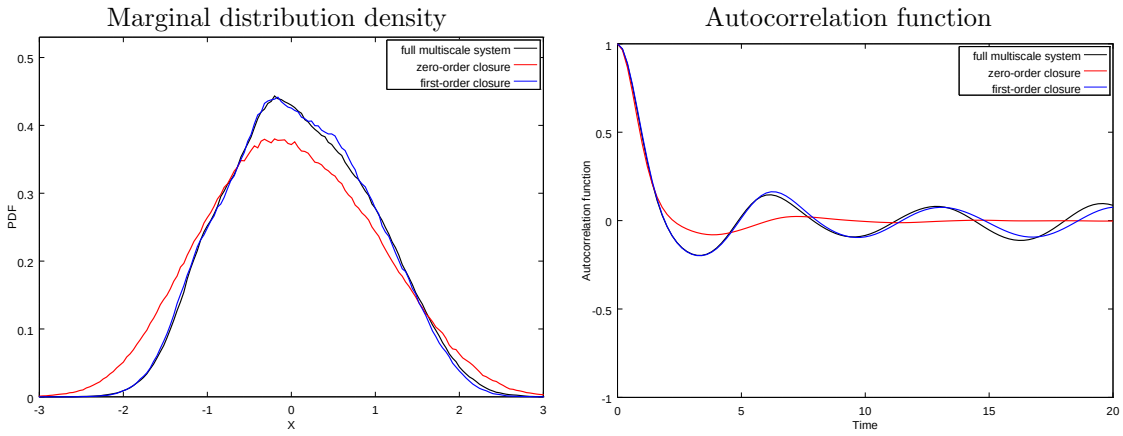

$F_x = 16, \quad \varepsilon = 0.1$

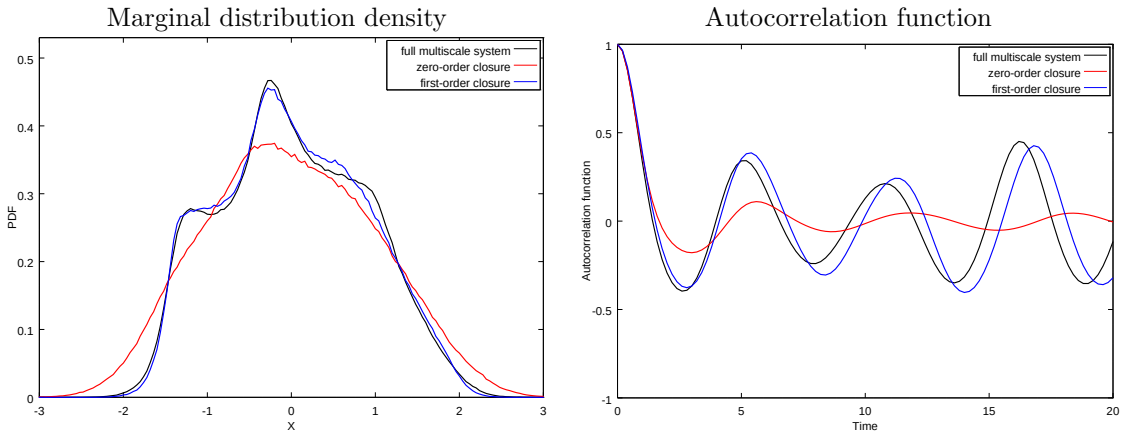

$F_x = 8, \quad \varepsilon = 0.1$

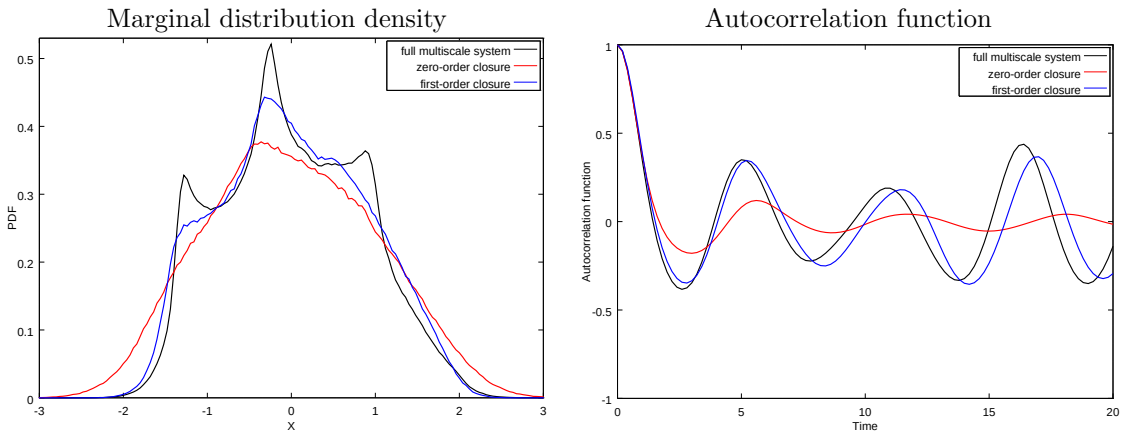

$F_x = 8, \quad \varepsilon = 0.01$

Figure 1. Marginal distribution densities and autocorrelation functions of slow variables.

This metric has the particularly intuitive property that the earth mover's distance between two delta distributions δ_α and δ_β is simply the distance between their centers $|\alpha - \beta|$.

Figure 2 shows distances between reduced systems DDFs and the corresponding multiscale slow variable DDFs. A variety of regimes is considered, with coupling parameters $\lambda_x, \lambda_y \in [0.1, 1]$, forcing parameters $F_x \in \{6, 7, 8, 10, 16\}$ and $F_y \in \{8, 12, 16\}$, and timescale separations $\varepsilon \in \{10^{-1}, 10^{-2}\}$. The data points are plotted with respect to coupling parameter λ_x. For each regime considered, the corresponding distances are shown for both zero-order and first-order reduced systems.

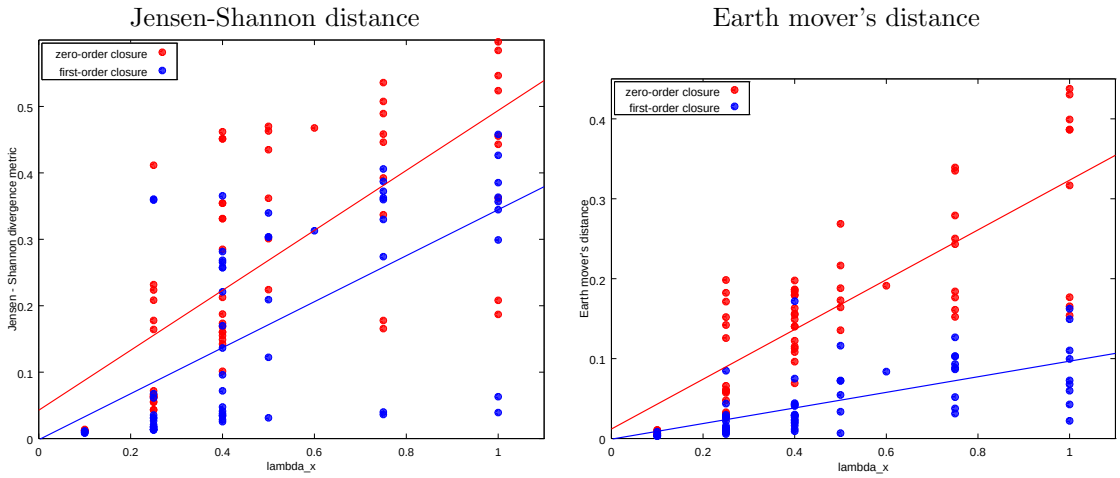

Figure 2. Distances between DDFs of reduced and multiscale systems, with linear best fit for the zero-order system (dashed line) and first-order system (solid line).

As the coupling strength between fast and slow systems increases, it is apparently more difficult for the reduced systems to capture the correct slow dynamics of the multiscale system. When plotted against λ_y, the coupling parameter for the fast system, this correlation is slightly weaker. Nevertheless, the distribution densities of the multiscale system are consistently closer in both metrics to the first-order reduced system than to the zero-order system.

7.2 Statistical comparison for L96 with nonlinear coupling

In this section we make statistical comparison of reduced models implementing the averaging methodology for nonlinear couplings of Section 4.5. We compare marginal distribution densities and autocorrelation functions of the slow variables in the full system and in both first- and zero-order reduced systems. As we see in Figure 3 and Figure 4, for certain parameter regimes we have close agreement but for others the differences can be much larger.

In particular, extra consideration must be taken with this system because here the parameters c, d control the damping in a significant manner, and depending on the regime d can have a significant effect on the forcing. If the fast limiting system is pushed into a regime with a highly non-Gaussian distribution, the quasi-Gaussian FDT calculation in the first-order reduced model will fail to produce an accurate coupling response. In more extreme cases with large contributions from the higher order terms, Figure 5, the limitations of both reduced order methods become apparent.

Using the metrics introduced in 7.1 we can explore the parameter space and find the limits of the model reduction method. shows distances between reduced systems DDFs and the corresponding multiscale slow variable DDFs. A multitude of regimes is considered, with coupling

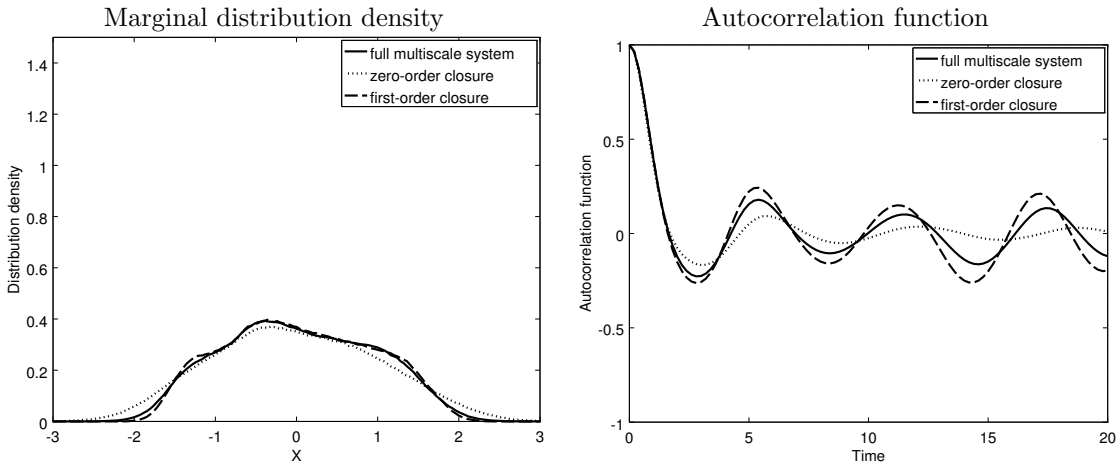

$F_x = 8,\ \lambda_x = \lambda_y = 0.4,\ a = 0,\ b = 1,\ c = 0,\ d = 0,\ \varepsilon = 0.1$

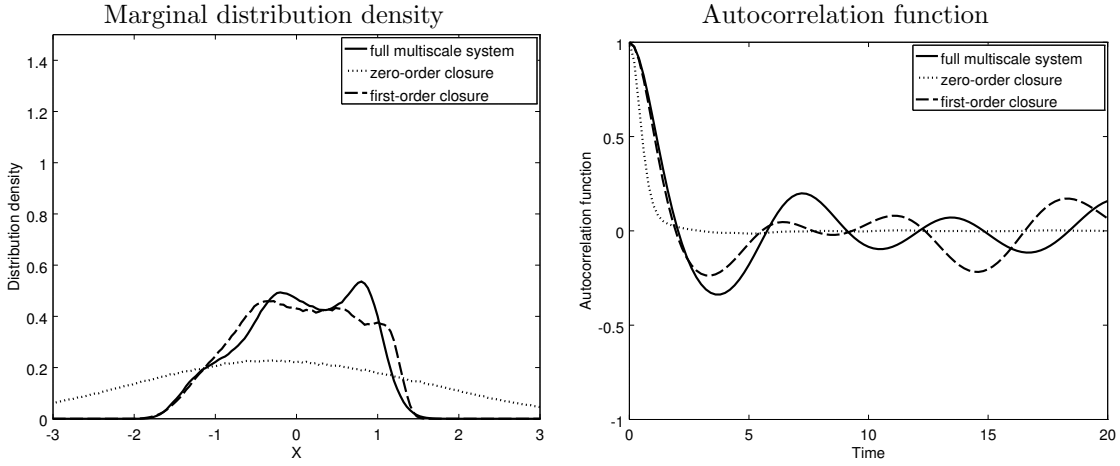

$F_x = 16,\ \lambda_x = \lambda_y = 0.3,\ a = 1,\ b = 1,\ c = 0.5,\ d = 0.5,\ \varepsilon = 0.1$

Figure 3. Marginal distribution densities and autocorrelation functions of slow variables.

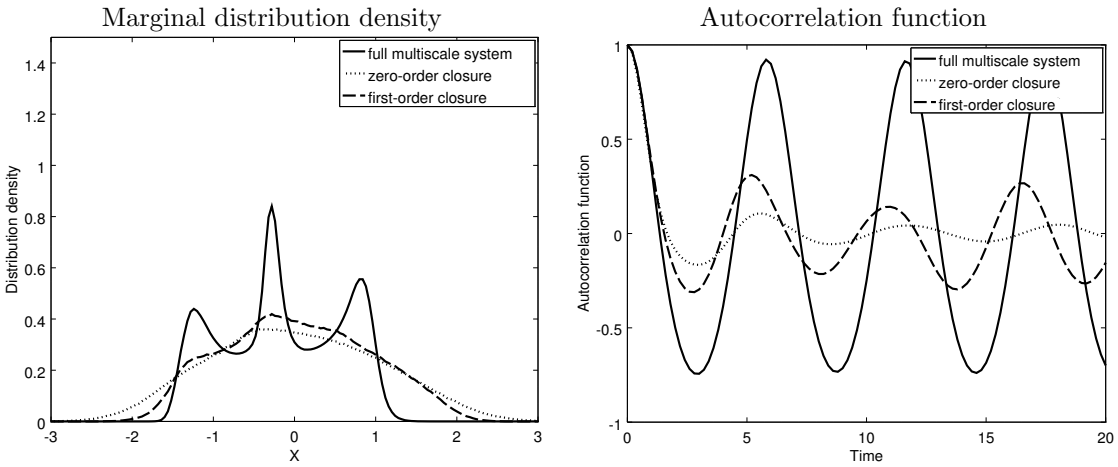

$F_x = 8,\ \lambda_x = \lambda_y = 0.4,\ a = 0,\ b = 0,\ c = 0.5,\ d = 0,\ \varepsilon = 0.1$

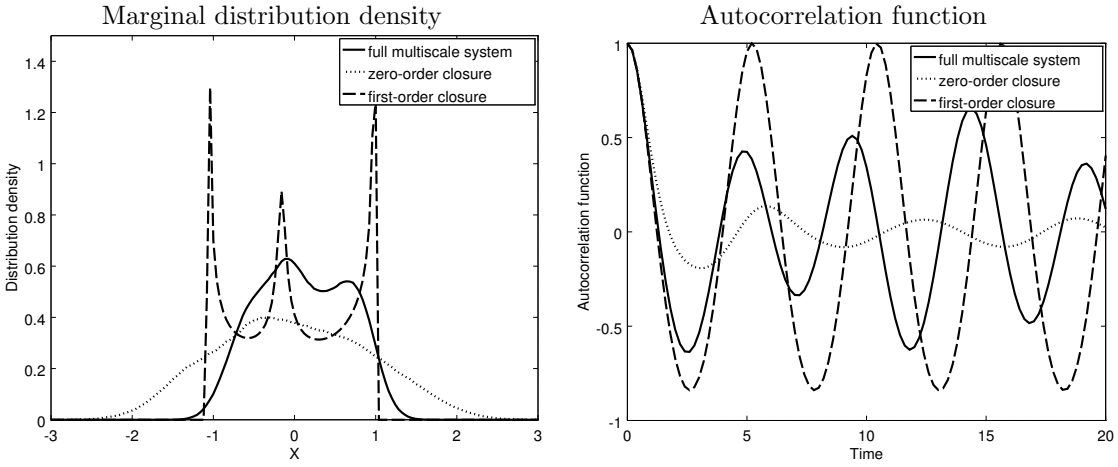

$F_x = 8,\ \lambda_x = \lambda_y = 0.4,\ a = 1,\ b = 0,\ c = 0.5,\ d = 0,\ \varepsilon = 0.1$

Figure 4. Marginal distribution densities and autocorrelation functions of slow variables.

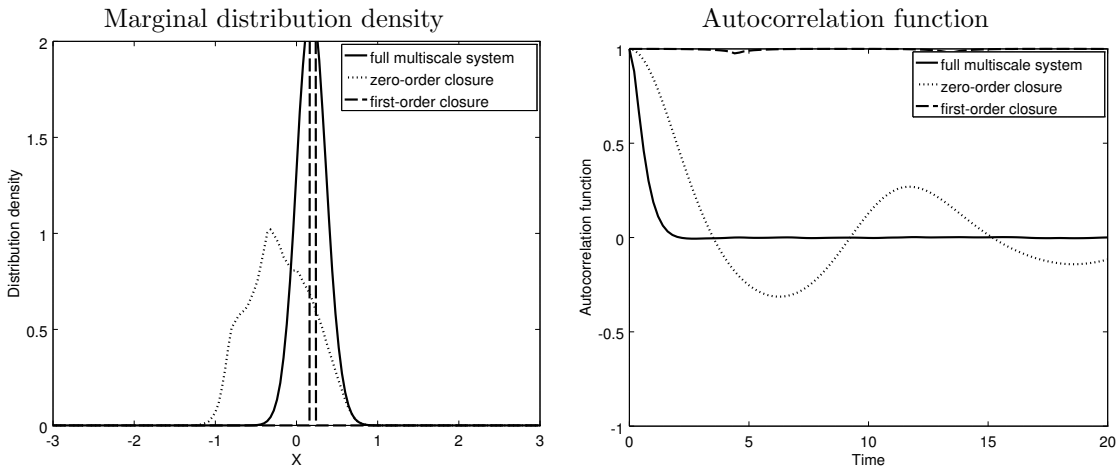

$F_x = 16,\ \lambda_x = \lambda_y = 0.4,\ a = 1,\ b = 0,\ c = 1,\ d = 0,\ \varepsilon = 0.1$

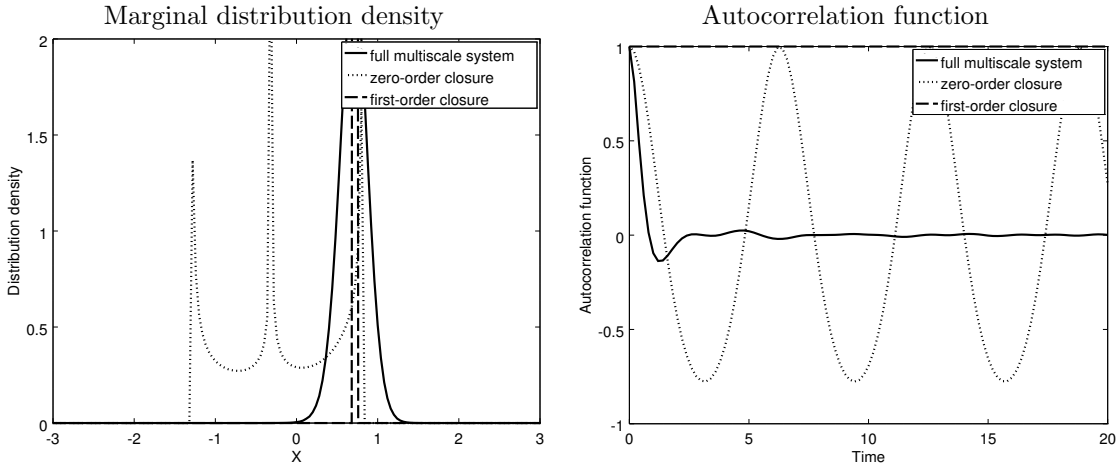

$F_x = 8,\ \lambda_x = \lambda_y = 0.4,\ a = 1,\ b = 1,\ c = 0.5,\ d = 0.5,\ \varepsilon = 0.1$

Figure 5. Marginal distribution densities and autocorrelation functions of slow variables.

parameters $\lambda_x = \lambda_y \in \{0.3, 0.4\}$, $a \in \{0, 1\}$, $b \in \{0, \pm 0.5, \pm 0.8, \pm 1\}$, $c \in \{0, \pm 0.3, \pm 0.5, \pm 1\}$, $d \in \{0, \pm 0.3, \pm 0.5, \pm 1\}$; forcing parameters $F_x \in \{6, 8, 16\}$ and $F_y = 12$; and timescale separations $\varepsilon \in \{10^{-1}, 10^{-2}\}$. The distances between distribution functions with respect to the Jensen-Shannon metric and Earth mover's distance are shown in Figure 6 For each parameter regime considered, distances from the full system distribution to the zero-order and first-order reduced systems are shown. Due to the high dimensionality of the parameter space and the low dimensionality of this ink, the horizontal component of each data point is determined by projecting the standardized parameter vector onto the 1-dimensional direction in parameter space with the highest observed correlation with the distances vector. This is equivalent to the method of partial least squares regression. (41)

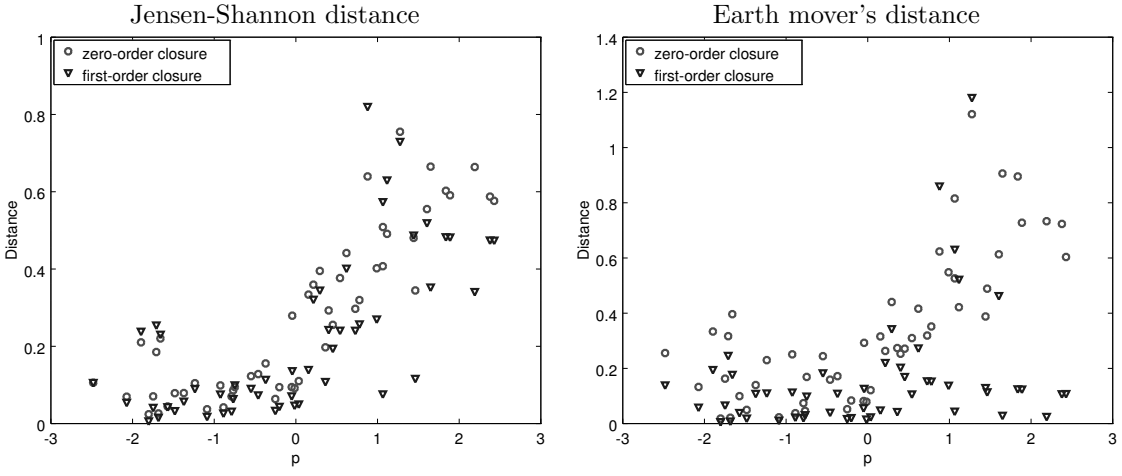

Figure 6. Distances between DDFs of reduced and multiscale systems for Lorenz 96 systems with nonlinear coupling

The coefficients of $\boldsymbol{v}_1$ are all positive, so increasing the value of a parameter typically will make the marginal distributions of a system more difficult to approximate using a reduced model. The parameters most highly correlated with a poorly-matched distribution are c, d, and λ_x, in that order. In any case, the first-order reduced model typically produces better approximations to the marginal distribution density function than the zero-order model.

CHAPTER 8

COMPARISON OF RESPONSE TO FORCING PERTURBATIONS

For a reduced model to be a useful approximation it should also respond in a similar way to perturbations. In Chapter 5 we outline the criteria for the response of an averaged model to be appropriately close to the response of the multiscale model, and in this section we present experimental results of perturbation response in the Lorenz 96 system. In particular we examine the response of the mean state $\langle \boldsymbol{x} \rangle$ of the slow variables, that is $b(\boldsymbol{x}) = \boldsymbol{x}$ in (Equation 5.4), in the Lorenz 96 system following perturbations by simple forms of external forcing. [1]

The two forms of forcing we consider are:

1. Heaviside step forcing

$$\boldsymbol{\delta f}_{\mathrm{H}}(t) = \begin{cases} \boldsymbol{v} & \text{if } t > 0, \\ 0 & \text{if } t < 0, \end{cases} \tag{8.1}$$

2. Ramp forcing

$$\boldsymbol{\delta f}_{r}(t) = \begin{cases} \boldsymbol{v} & \text{if } t > t_r, \\ \boldsymbol{v}t/t_r & \text{if } 0 < t < t_r, \\ 0 & \text{if } t < 0, \end{cases} \tag{8.2}$$

---

[1] Material in this chapter has been submitted for publication and is awaiting review.(34)

where $\boldsymbol{v}$ is a constant vector and t_r is a fixed time when the ramp forcing reaches its maximum. To compute the response of the mean state which we denote by $\delta\langle \boldsymbol{x} \rangle(t)$, corresponding to $b(\boldsymbol{x}) = \boldsymbol{x}$ in (Equation 5.5), we first generate an initial ensemble of 10^4 members sampled from a single trajectory which has been given sufficient time to settle onto the attractor. Exploiting the translational symmetry of the Lorenz 96 system, the ensemble size is increased by a factor of N_x by rotating the indices of each member.

For each ensemble member we compute a short trajectory under the unperturbed dynamics as well as the under the perturbed dynamics, then we take the difference between these two trajectories and average over the entire ensemble. We restrict our attention to forcing at a single slow variable, $\boldsymbol{v} = \delta f \cdot \hat{e}_j$, where δf is a scalar and $\hat{e}_j$ a standard basis vector in $\mathbb{R}^{N_x}$, motivated in part by our expectation that the response will be close to linear for small forcing and short times. Taking advantage of the translation invariance of the Lorenz 96 system we only consider forcing at a single node.

The initial calculations required to generate the reduced Lorenz 96 system take only a few minutes on a modern laptop; once computed, numerical simulation of the reduced system is faster than the multiscale system by a factor of ε^{-1}. Computing the mean response for a single forcing for 5 time units with a sufficiently large ensemble size (10^5 trajectories) takes over an hour in the multiscale system with $\varepsilon = 10^{-2}$ but less than three minutes for the corresponding reduced system.

8.1 Perturbation response for L96 with linear coupling

The plots in Figure 7 show the response of the slow variables mean state $\delta\overline{\boldsymbol{x}}$ to Heaviside forcing of magnitudes $\delta f = 0.01$ and $\delta f = 1$ at node x_{11} for five time units, averaged over an ensemble of 200,000 trajectories. For comparison, the average magnitude of the right hand side for this parameter regime is $\langle|\frac{\mathrm{d}\boldsymbol{x}}{\mathrm{d}t}|\rangle = \langle|\boldsymbol{F}|\rangle = 0.38$.

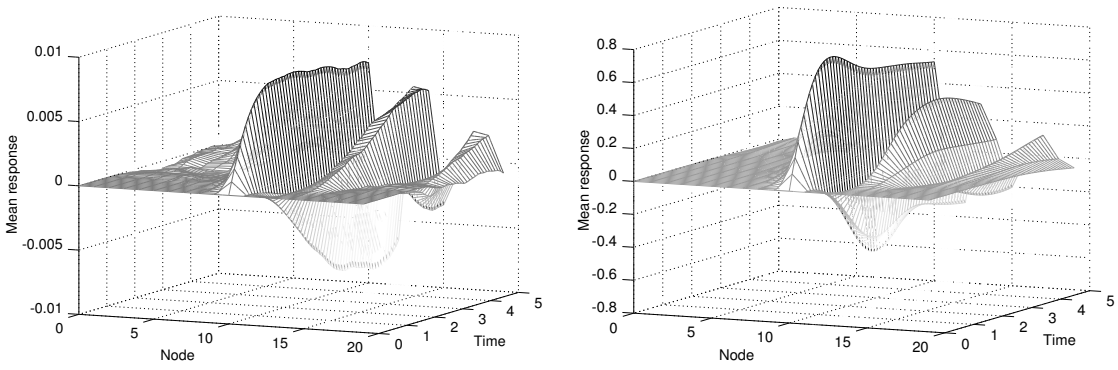

Figure 7. Response of $\langle\boldsymbol{x}\rangle$ ($b(\boldsymbol{x}) = \boldsymbol{x}$ in (Equation 5.5)) to Heaviside step forcing $\delta f = 0.01$ (left) and $\delta f = 1$ (right) at node x_{11} in a chaotic regime of the two-time rescaled Lorenz 96 system. $F_x = 16,\ F_y = 12,\ \lambda_x = 0.4,\ \lambda_y = 0.4,\ \varepsilon = 0.1$

In these plots we can see the primary response in the forced node as well as the propagation of the response to the adjacent nodes in the direction of advection. Here the large features of the Heaviside forcing mean response are present after five time units and provide a good indication of the infinite time response.

We now compare the mean response of the full and reduced systems. Figure 8 and Figure 9 show snapshots of the mean responses for the two-scale and reduced models at times $t = 2$ and $t = 5$ with the Heaviside forcing of $\delta f = 0.01$ and $\delta f = 1$, respectively. Response to ramp forcing is shown in Figure 10 and Figure 11, where the forcing increases linearly from zero for $t_r = 3$ time units to a maximum of $\delta f = 0.01$ and $\delta f = 1$, respectively. In all these plots, the reduced models capture quite closely the response of the node which is directly perturbed, but they differ in their ability to capture the responses of the remaining nodes. In the case of larger forcing $\delta f = 1$, the first order model responds closely to the multiscale system, while the zero order model tends to underrepresent the response. When the forcing is small, the small oscillations that propagate in the multiscale system are relatively large compared to the linear response, and this is a purely multiscale phenomena that the reduced models are unable to capture. Note that this difference is less prominent as the timescale separation increases ($\varepsilon \to 0$), allowing sufficient time for the oscillations to dissipate in the strongly mixing fast system.

For a quantitative comparison of these responses, we plot versus time the relative error

$$\frac{\|\delta\overline{\boldsymbol{x}}(t) - \delta\overline{\boldsymbol{x}}_A(t)\|}{\|\delta\overline{\boldsymbol{x}}(t)\|} \tag{8.3}$$

and the cosine similarity

$$\frac{\delta\overline{\boldsymbol{x}}(t) \cdot \delta\overline{\boldsymbol{x}}_A(t)}{\|\delta\overline{\boldsymbol{x}}(t)\| \cdot \|\delta\overline{\boldsymbol{x}}_A(t)\|} \tag{8.4}$$

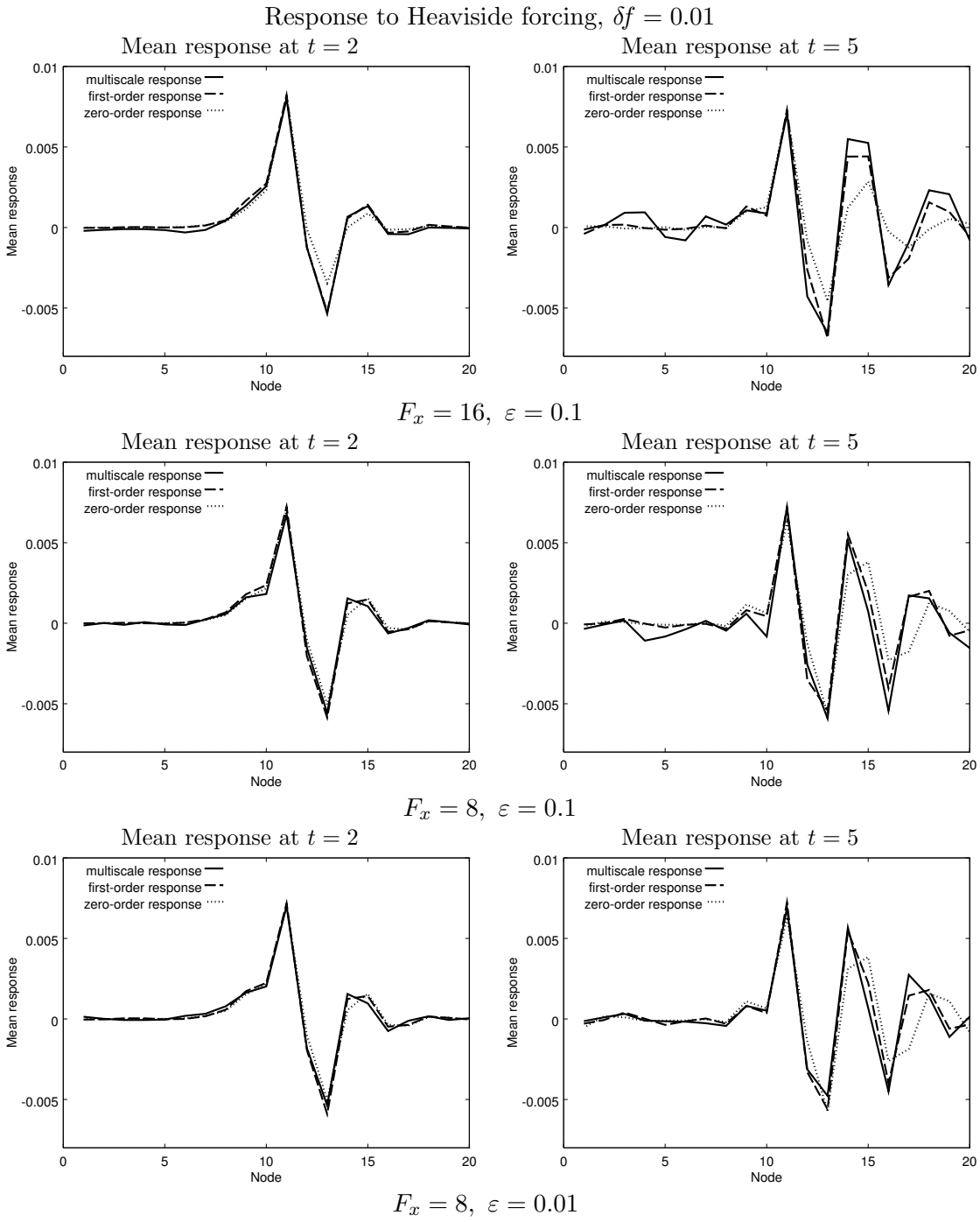

Figure 8. Snapshots of the mean response $\delta\overline{\boldsymbol{x}}(t)$ to small Heaviside forcing

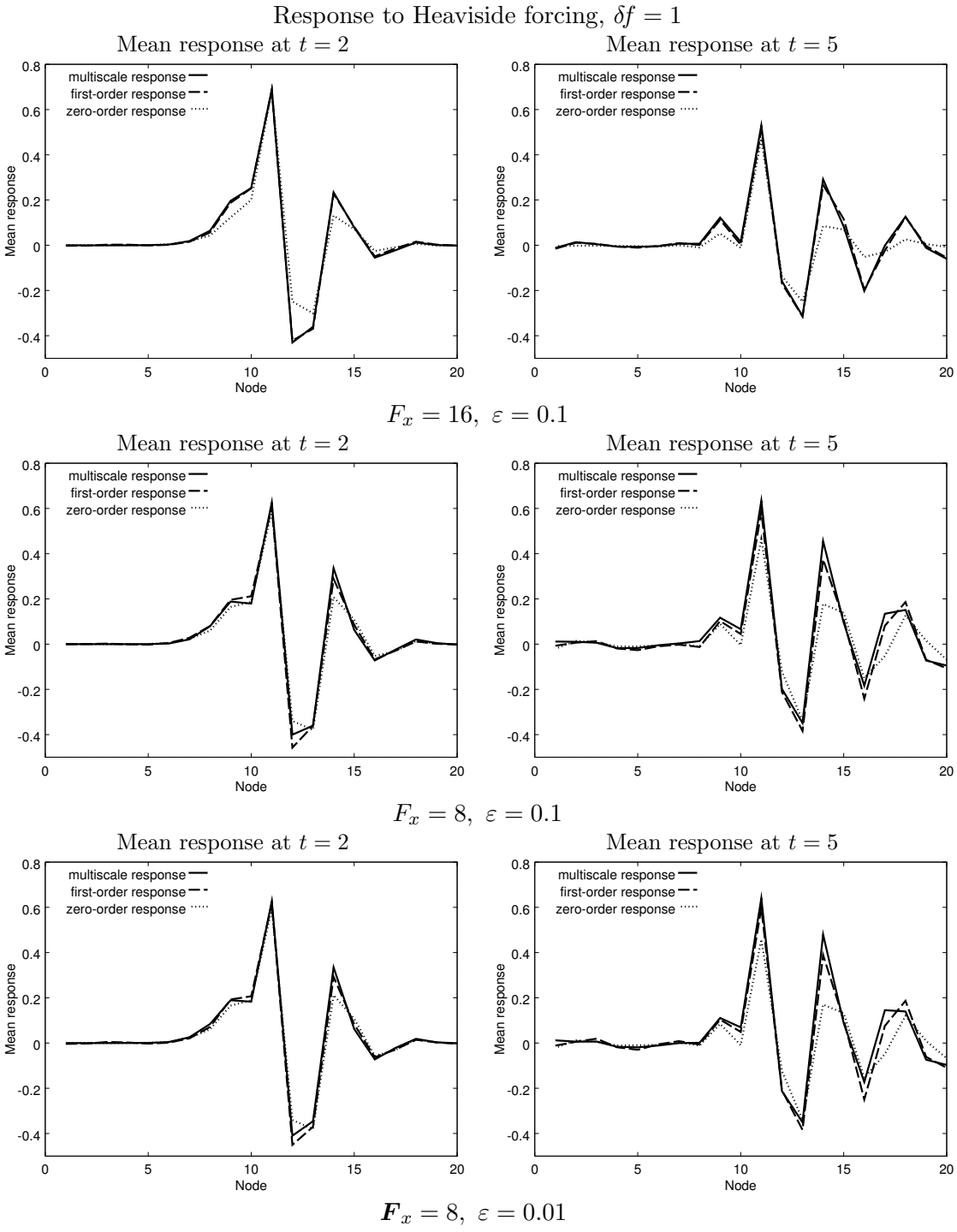

Figure 9. Snapshots of the mean response $\delta\overline{\boldsymbol{x}}(t)$ to large Heaviside forcing

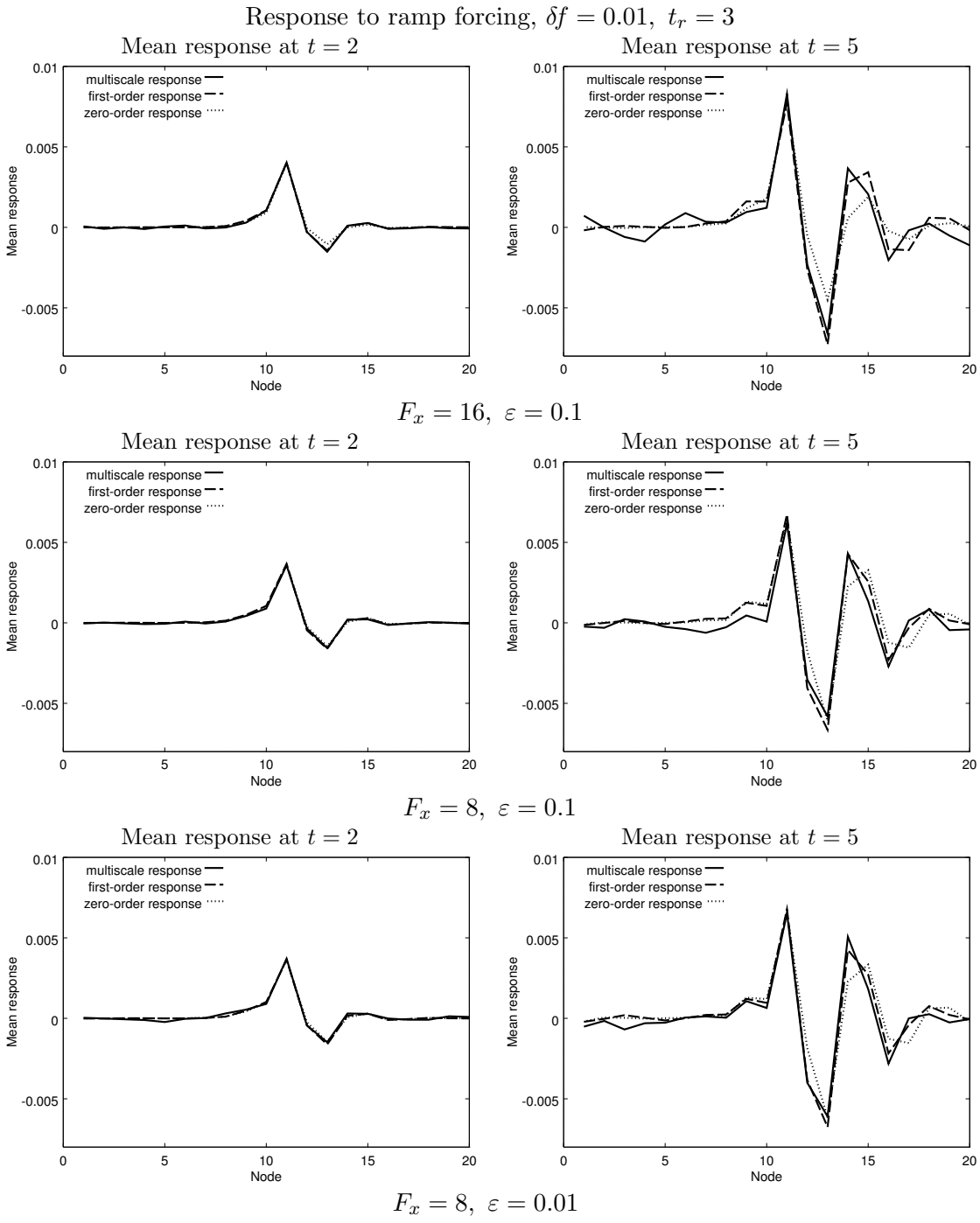

Figure 10. Snapshots of the mean response $\delta\overline{\boldsymbol{x}}(t)$ to small ramp forcing

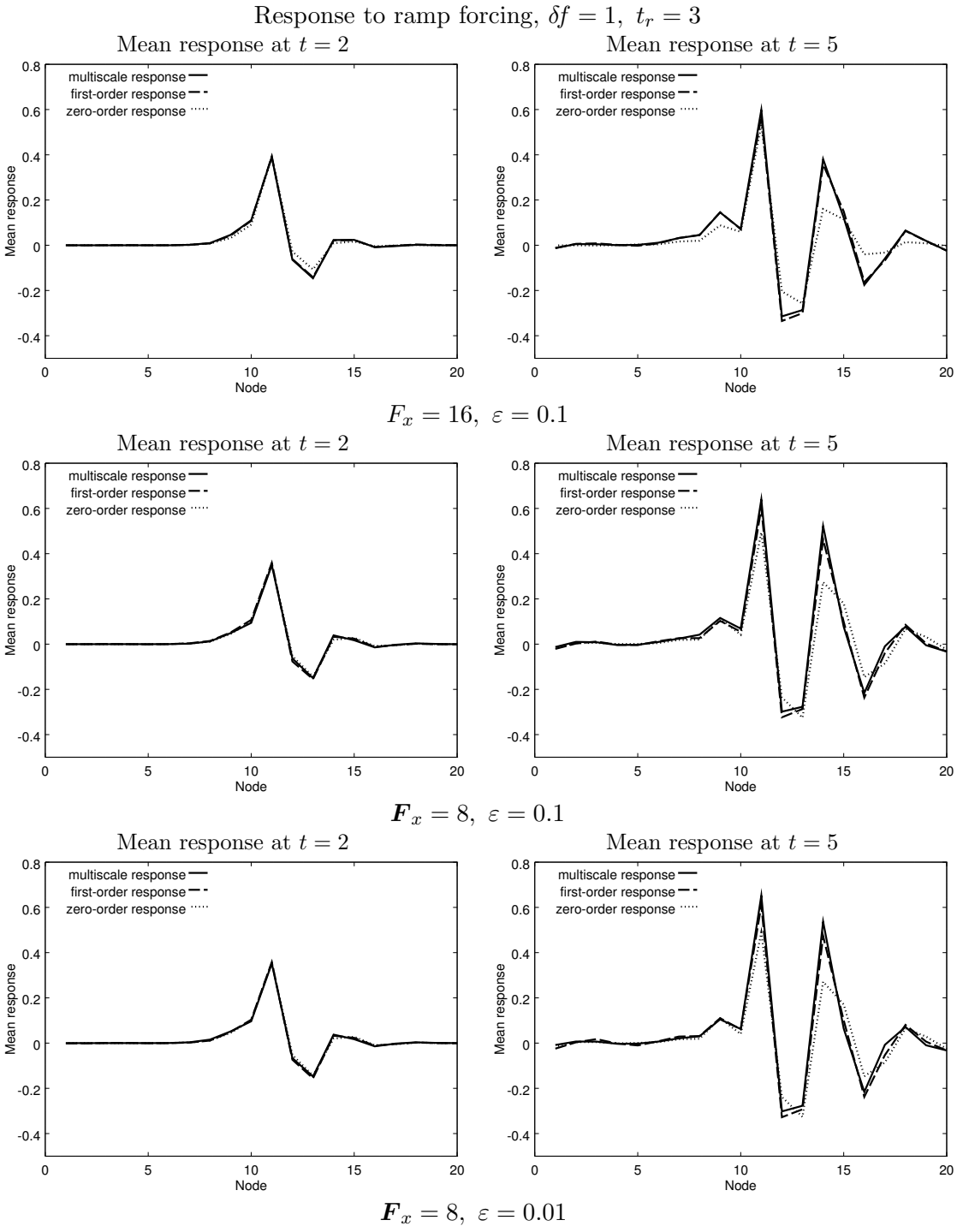

Figure 11. Snapshots of the mean response $\delta\overline{\boldsymbol{x}}(t)$ to large ramp forcing

of the mean responses $\delta\overline{\boldsymbol{x}}(t)$ and $\delta\overline{\boldsymbol{x}}_A(t)$ of the multiscale and reduced systems, respectively. These plots are shown in Figure 12 – Figure 15 for first-order and zero-order reduced systems.

We observe that the first-order reduced system response is a much closer approximation to the multiscale response than the corresponding zero-order response in all cases. In these regimes the relative error of the first-order response is limited to about 30% for small forcings and about 20% for the ramp forcing, while in the zero-order system the difference can exceed 50% at $t = 5$.

Remark the plots for small ramp forcing in Figure 14, where we see a spike in the response differences shortly after the onset of forcing in the weakly chaotic regime ($F_x = 8, F_y = 12$) with large timescale separation ($\varepsilon = 0.01$) in the multiscale system. In this regime the small nonlinear fluctuations of the multiscale system develop rapidly and are relatively large compared to the ramp forcing for t near zero, so the relative error of the reduced system responses is large. As the ramp forcing increases, the large features of the response become manifest and the nonlinear contribution becomes negligible.

8.2 Perturbation response for L96 with nonlinear coupling

In Figures Figure 16 and Figure 17 we see the response of the slow variables mean state $\delta\overline{\boldsymbol{x}}$ to Heaviside forcing at node x_{11} for five time units, averaged over an ensemble of 20,000 trajectories. The two parameter regimes shown correspond to the regimes in Figure 3.

Response to small Heaviside forcing, 1% of the average magnitude of $|\frac{\mathrm{d}\boldsymbol{x}}{\mathrm{d}t}|$, is shown in Figure 16. Here the relative errors are quite large, due to the size of the nonlinear effects compared to the linear response - note that the vertical scales of these plots are $[0, 1]$ but

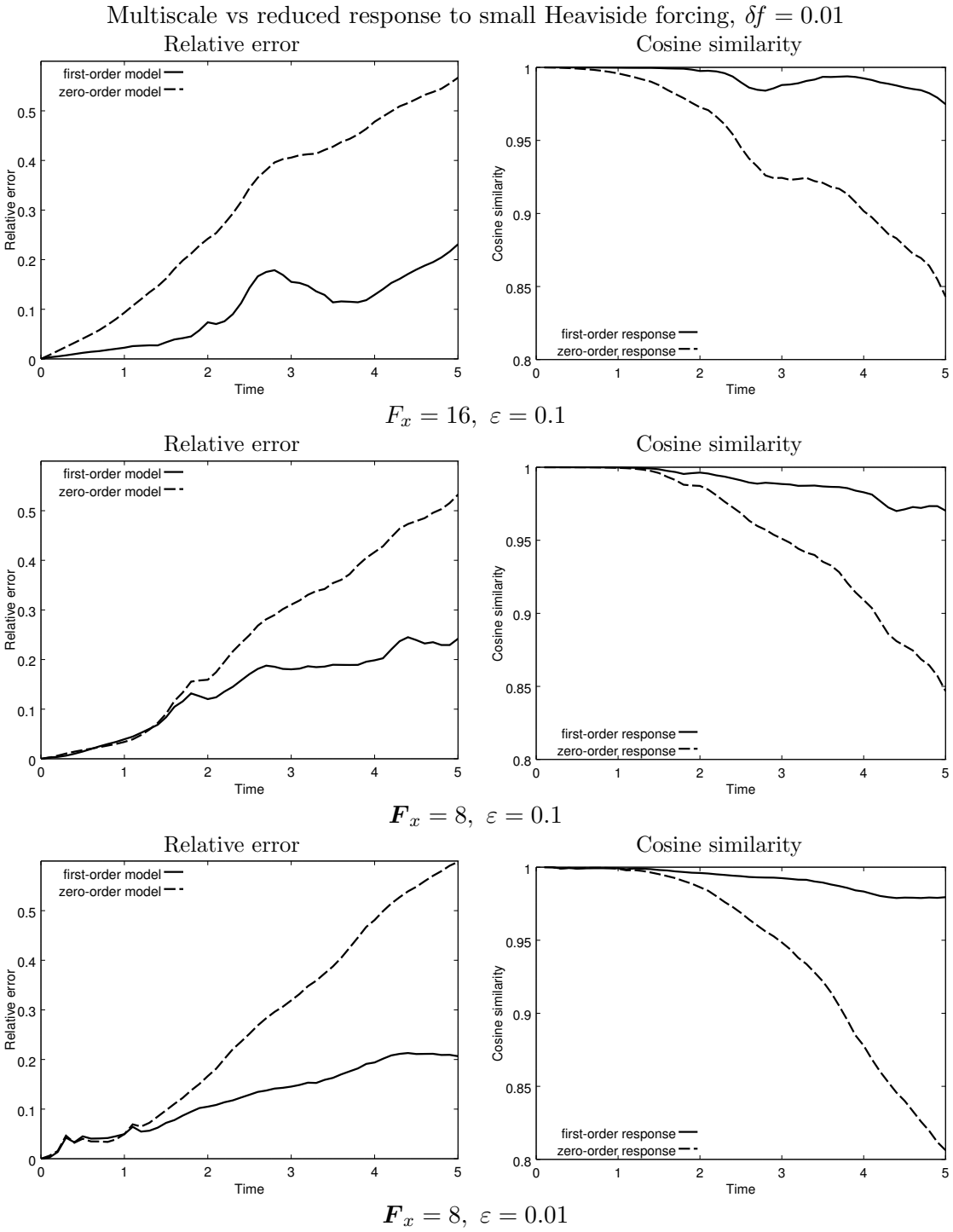

Figure 12. Comparison of multiscale and reduced system mean responses $\delta\overline{\boldsymbol{x}}(t)$ to small Heaviside forcing using relative distance (Equation 8.3) and cosine similarity (Equation 8.4).

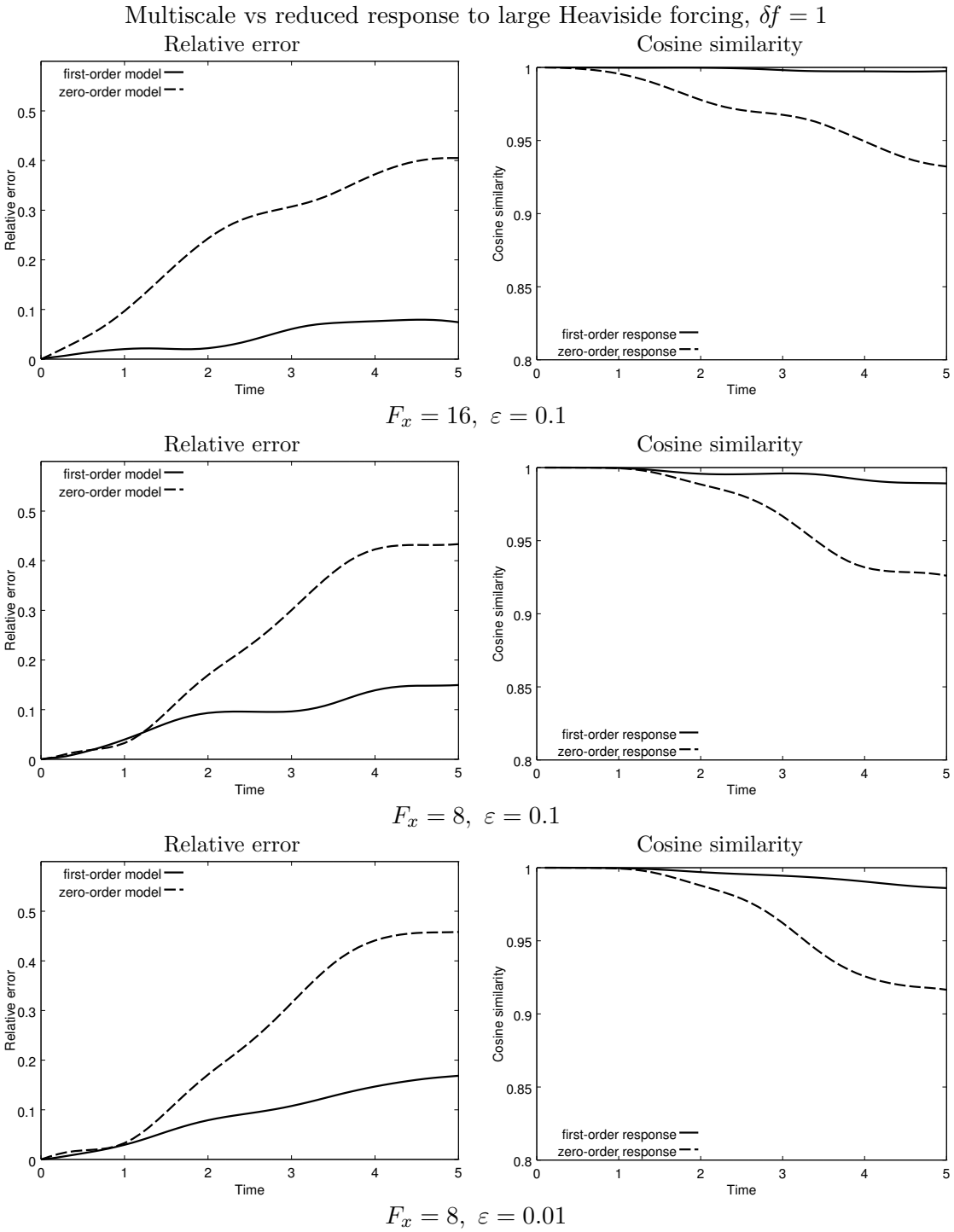

Figure 13. Comparison of multiscale and reduced system mean responses $\delta\overline{\boldsymbol{x}}(t)$ to large Heaviside forcing using relative distance (Equation 8.3) and cosine similarity (Equation 8.4).

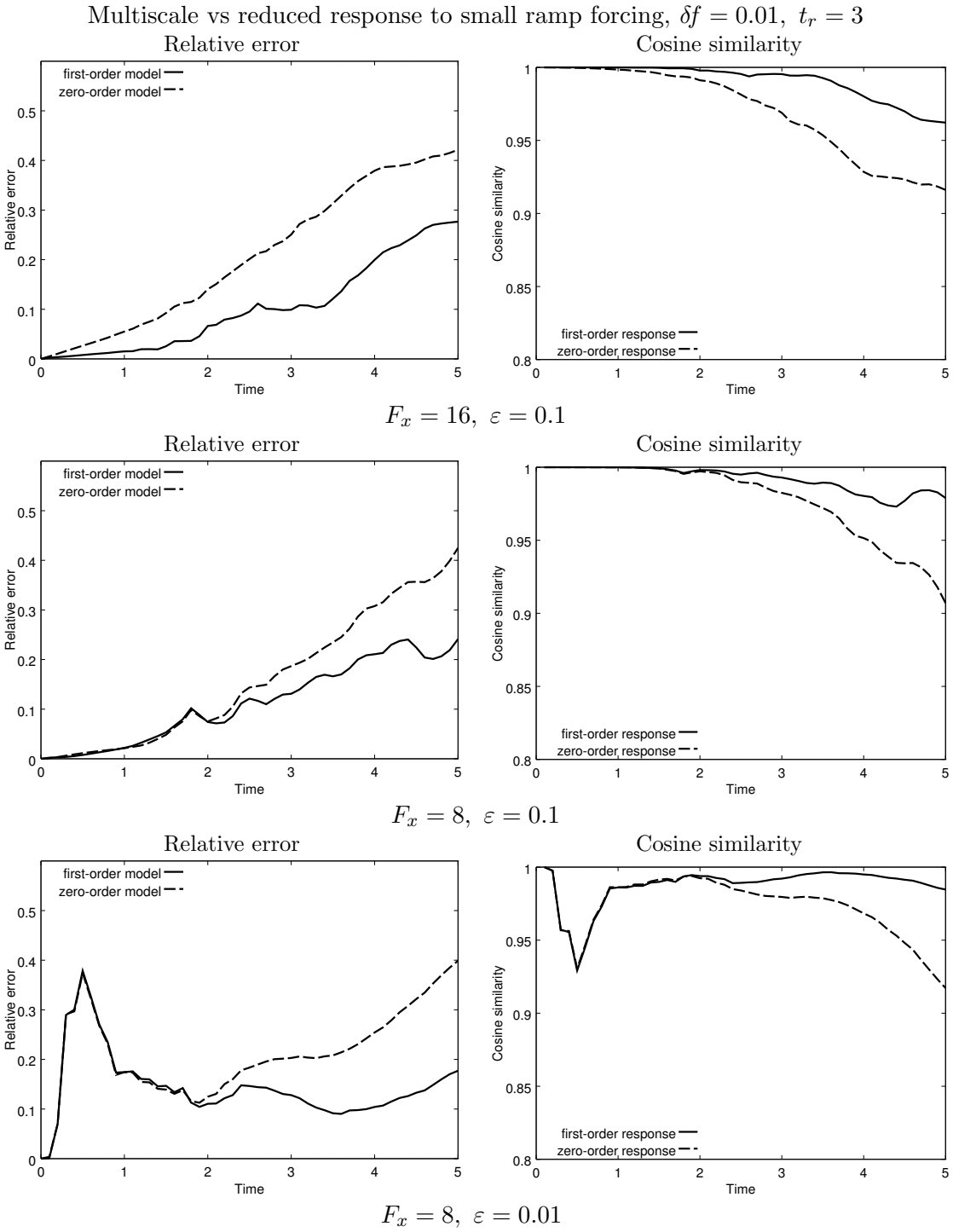

Figure 14. Comparison of multiscale and reduced system mean responses $\delta\overline{\boldsymbol{x}}(t)$ to small ramp forcing with $t_r = 3$ using relative distance (Equation 8.3) and cosine similarity (Equation 8.4).

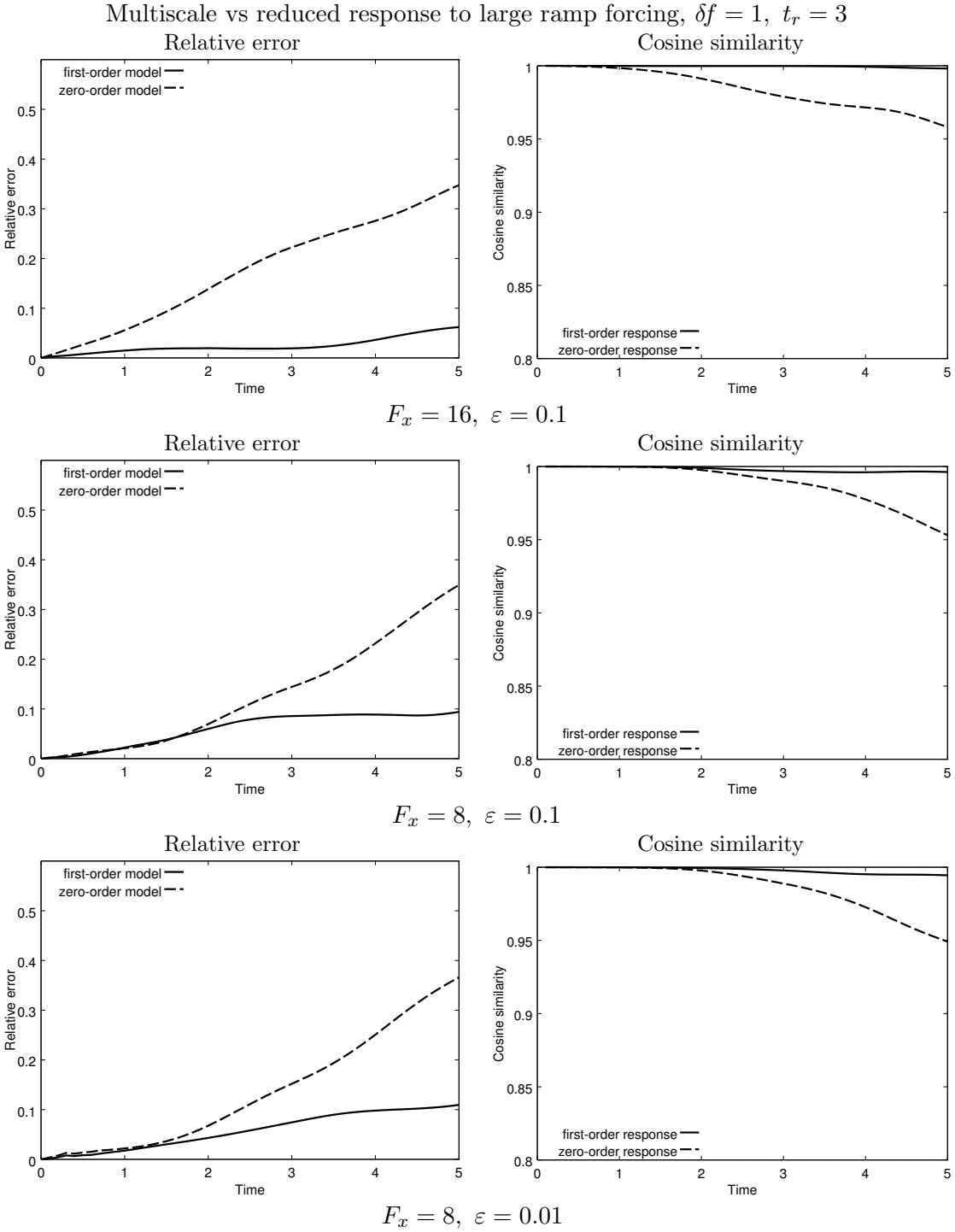

Figure 15. Comparison of multiscale and reduced system mean responses $\delta\overline{\boldsymbol{x}}(t)$ to large ramp forcing with $t_r = 3$ using relative distance (Equation 8.3) and cosine similarity (Equation 8.4).

the linear-coupling response comparisons above are plotted on $[0, 6]$ and $[0.8, 1]$, respectively. Response to large magnitude Heaviside forcing, on the order of $|\frac{\mathrm{d}\boldsymbol{x}}{\mathrm{d}t}|$ is shown in Figure 17, for which we see much lower relative errors which are comparable to the linear-coupling results.

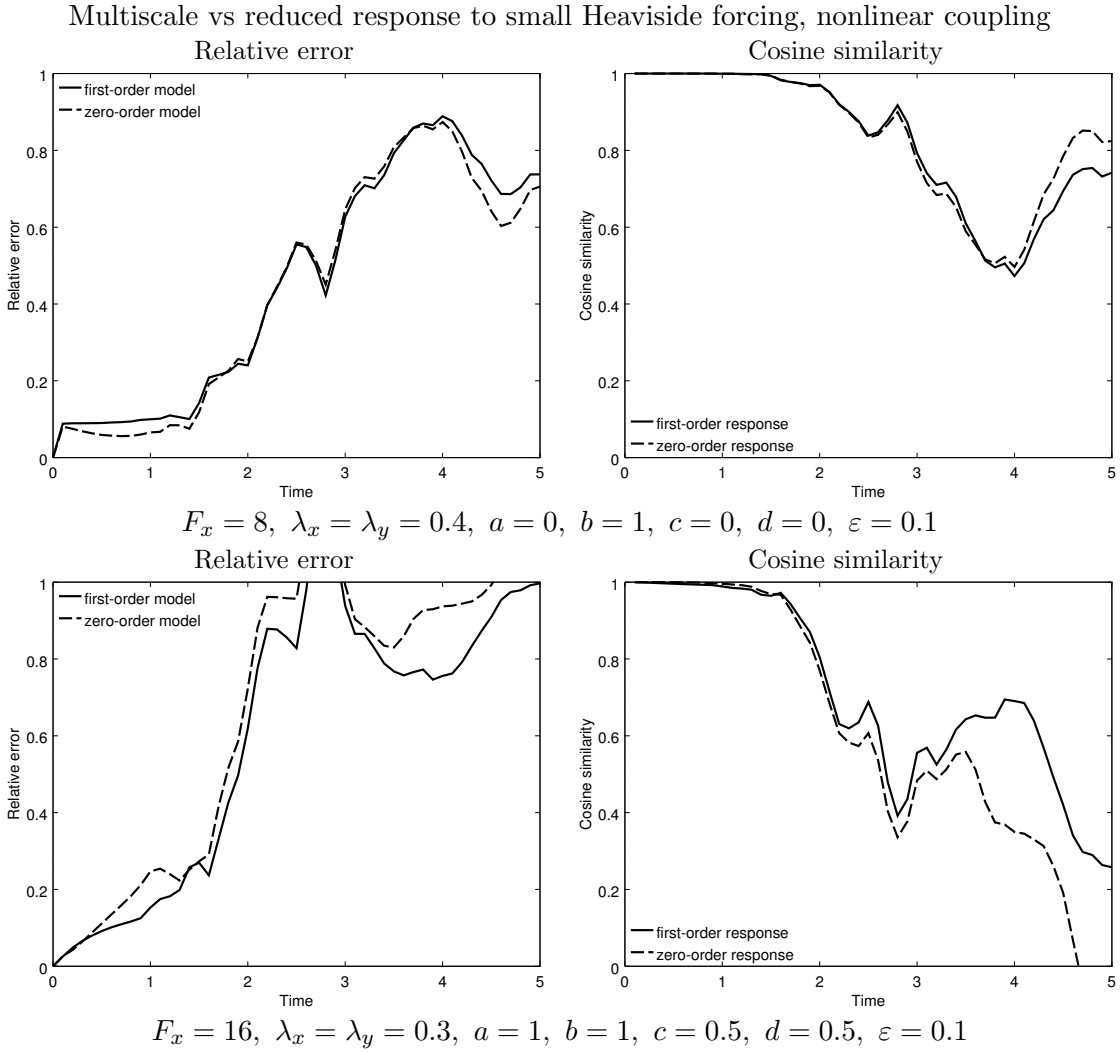

Figure 16. Comparison of multiscale and reduced system mean responses $\delta\overline{\boldsymbol{x}}(t)$ to small Heaviside forcing for Lorenz 96 system with nonlinear coupling.

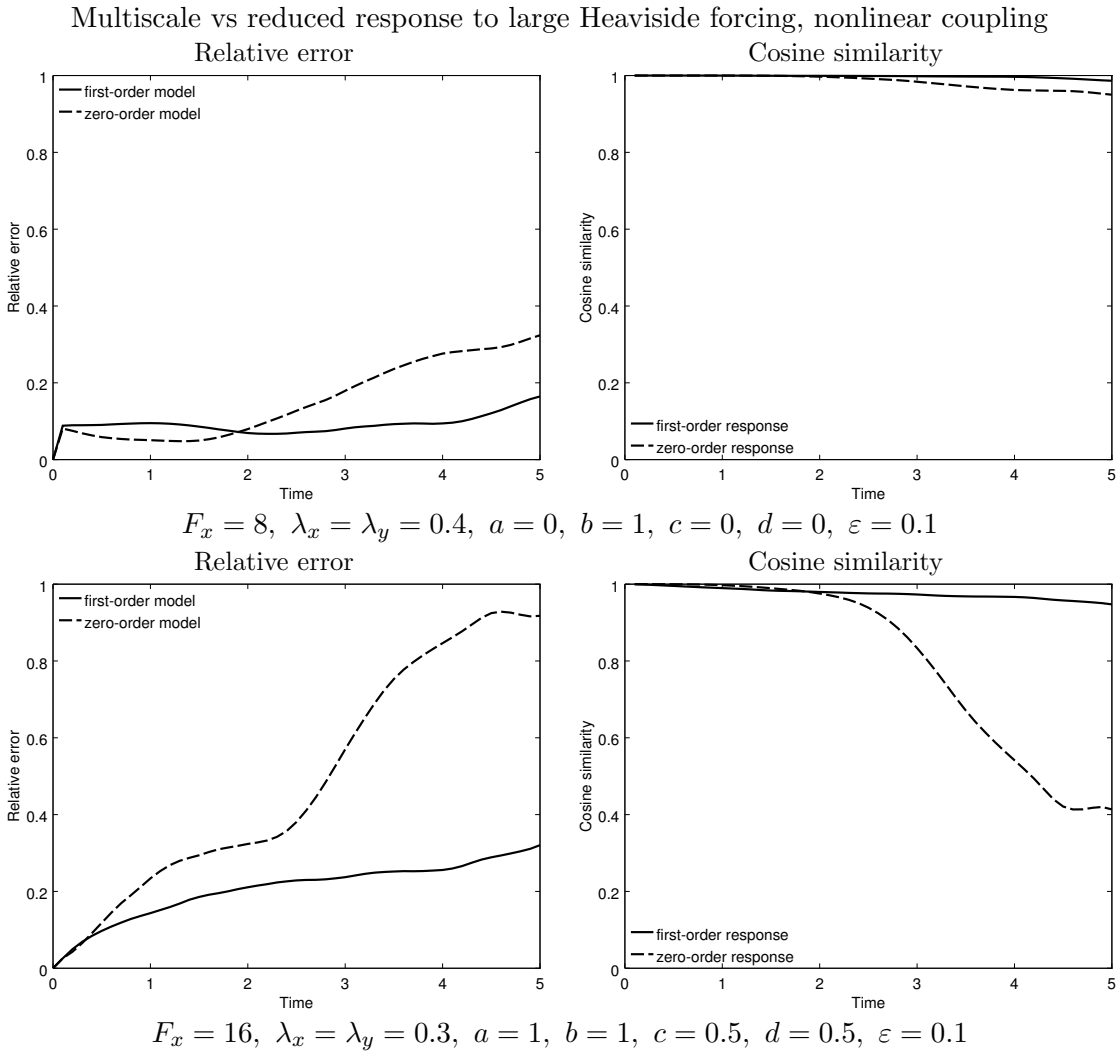

Figure 17. Comparison of multiscale and reduced system mean responses $\delta\overline{\boldsymbol{x}}(t)$ to large Heaviside forcing for Lorenz 96 system with nonlinear coupling.

CHAPTER 9

IDEAL RESPONSE

As we have seen from the FDT, the linear response operator of a system at equilibrium can be found using the long-time statistics of the unperturbed system. For a large multiscale system, it may be interesting to see how well its response operator can be approximated using the statistics of an appropriate reduced system; this would be especially important to know in the general case since we often hope to model multiscale physical reality using a reduced model, and we would hope they have similar perturbation response. In this chapter we will perform a more modest exploration of the approximation of the slow variables response in the two-timescale Lorenz 96 system (Equation 6.6) using the corresponding averaged system statistics.

In Chapter 8 we compare the observed responses of similar systems. However, in the context of the FDT it seems worth comparing the linear responses of these systems as well. If we recall, for a time-dependent additive forcing term $\boldsymbol{\delta f}(t)$ the mean linear response is computed as a convolution with a response kernel

$$\delta\overline{\boldsymbol{x}}(t) = \int_0^t R(t-\tau)\boldsymbol{\delta f}(\tau)\,\mathrm{d}\tau. \tag{9.1}$$

In the quasi-Gaussian approximation this operator is given by $R(t) = C(t)$, the autocorrelation function (Equation 3.26) of the unperturbed system. But how does this compare to the 'true'

linear response operator for this system? The linear response operator can be useful to know for a large system, since it would permit the estimation of responses to a wide variety of small perturbations without requiring significant computation. Knowing the linear response operator would perhaps be especially useful when the level of noise is large compared with the response, which would otherwise make extracting a statistically significant signal a difficult process (11). Furthermore, the linear response operator could be useful in solving the inverse problem to determine what external forcing is needed to produce a particular mean response.

Recall that for a constant (Heaviside) perturbation $\boldsymbol{\delta f}$ the linear response is given by

$$\delta\overline{\boldsymbol{x}}(t) = \mathcal{R}(t)\boldsymbol{\delta f}. \tag{9.2}$$

For the quasi-Gaussian FDT approximation, the linear response operator $\mathcal{R}$ is approximated by the integral of the autocorrelation function (Equation 3.26):

$$\mathcal{R}(t) = \int_0^t C(t)\,\mathrm{d}\tau. \tag{9.3}$$

To compare the actual linear response, we use the "ideal" response of Gritsun & Dymnikov (1999), which is computed as a linear least squares of the actual measured responses with respect to the forcing magnitudes (42; 19; 20; 21; 22; 23; 43; 44; 15). We see in Figure 18 the ideal responses for the multiscale and first-order reduced system for the chaotic parameter regime, $F_x = 16$. They are quite similar, which is to be expected as their marginal distributions and autocorrelation functions are very similar. How nonlinear is the actual response?

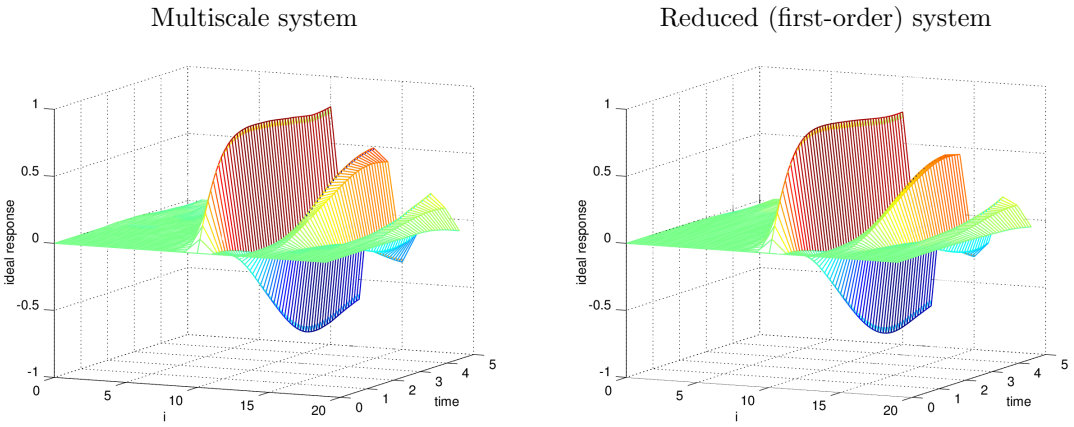

Figure 18. Ideal responses of multiscale and reduced (first order) system for Heaviside forcing at a single node. $F_x = 16,\ \varepsilon = 0.1$

In Figure 19 we show the relative error of the linear response and actual response for various magnitudes of forcing. We see that in the full system the smallest forcing result in the largest relative difference, likely due to the small nonlinearities which are magnified in this setting. For the reduced system the responses are all quite close to linear, where here the largest difference is seen for the largest forcing magnitudes.

In Figure 20 we compare response to Heaviside forcing in the multiscale system to FDT response computed using reduced system statistics. Snapshots of the response are shown at times $t = 2$ and $t = 5$. Of particular note is the poor performance of the first-order system FDT response, unusual because it performs well in other comparisons. However, this might be expected because the first-order system does not have a Gaussian distribution in these regimes (Figure 1), and thus an FDT quasi-Gaussian approximation may be inappropriate. The zero-

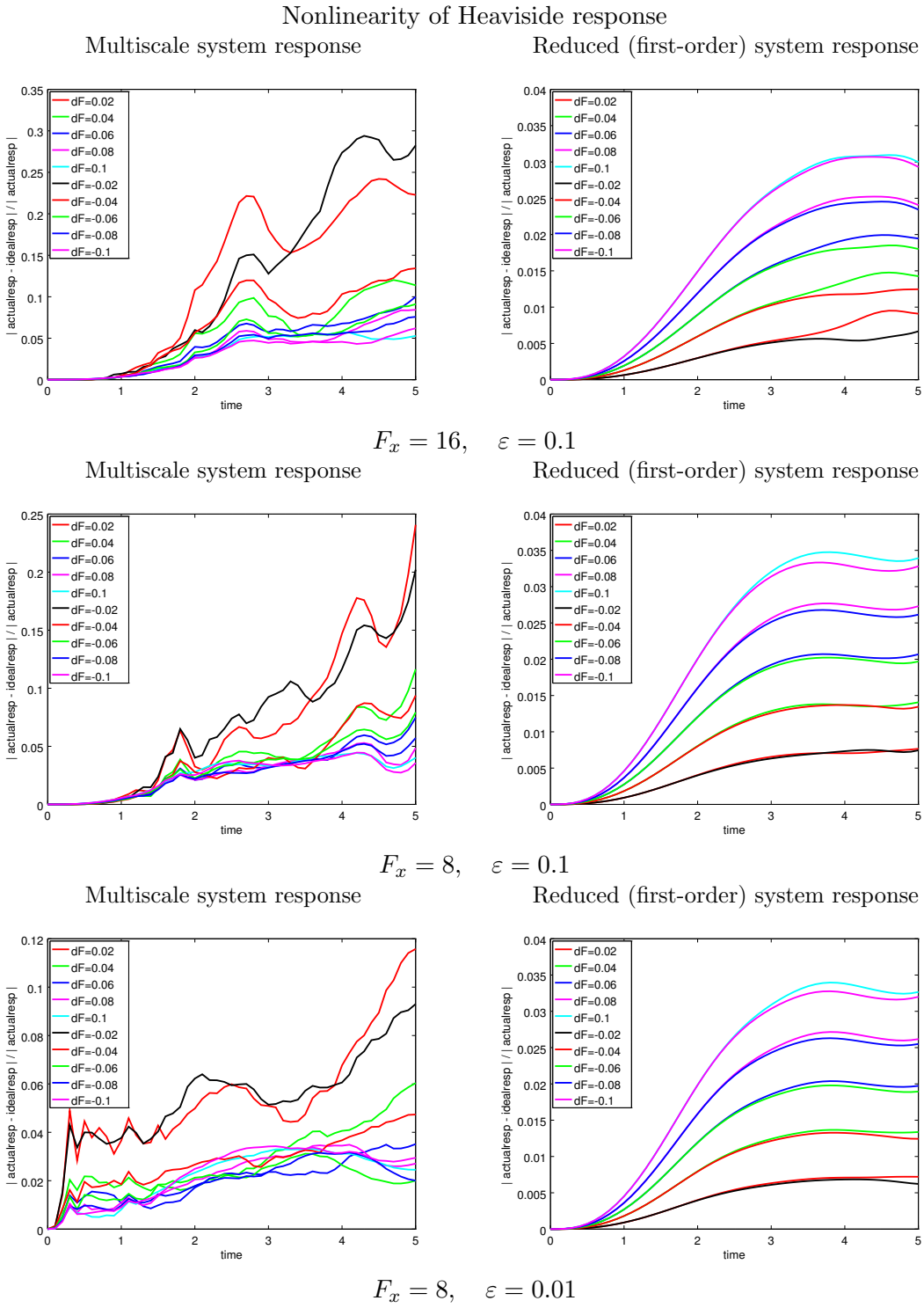

Figure 19. Relative difference of actual response and ideal response for Heaviside forcing at a single node

order systems, however, do have distributions which are close to Gaussian, and so their predicted FDT responses are closer to the actual response.

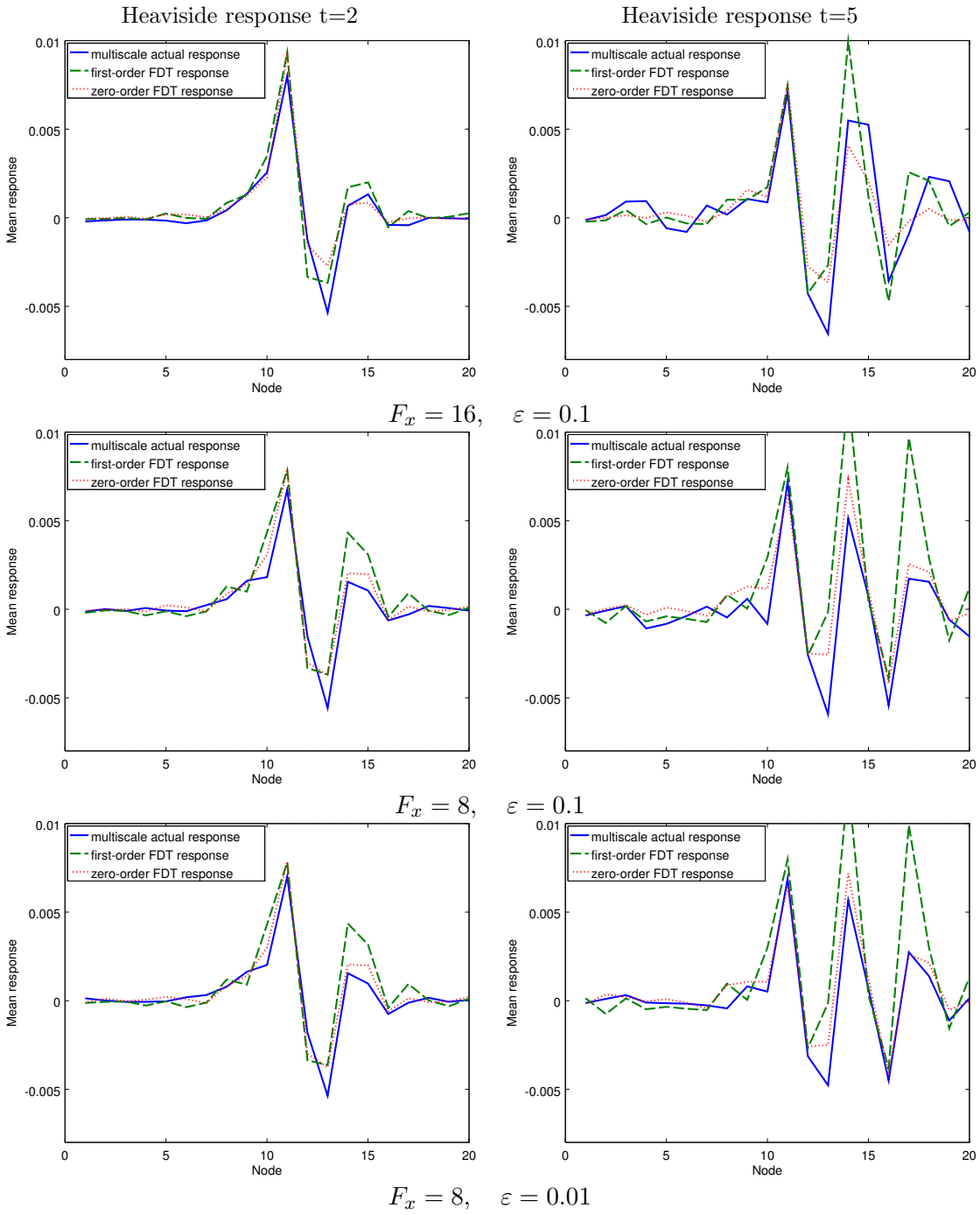

Figure 20. Response of multiscale system and FDT response of reduced systems for Heaviside forcing at a single node

CHAPTER 10

CONCLUSION

In this work we explored an application of the averaging method for the model reduction of two-timescale systems. We describe the general setting where this technique can be applied and describe practical implementation of the averaging method for systems with simple coupling terms. We find that the slow variables can be reasonably well represented using an averaged model computed on a single invariant manifold with a linear response correction term. For a range of parameter regimes, coupling types, and timescale separations, the reduced model provides reasonably good approximations of both long-time statistics and perturbation response in the slow variables at a fraction of the computational cost of the full system.

In our application to the Lorenz 96 system, the first-order reduced system was able to accurately capture the marginal distribution densities and autocorrelation functions of solutions and the mean response of the system to simple forcing perturbations,

Due to the greatly reduced computational demands of such reduced systems and the relative fidelity of the large features of the full system, this linear response closure approximation has potential practical utility for chaotic two-timescale systems as considered in this study, and perhaps warrants consideration when no better model reduction techniques are available.

For a more updated version of this document please contact the author at marc.kjerland@gmail.com.

APPENDICES

Appendix A

DERIVATION OF LINEAR RESPONSE FORMULA FOR A NONLINEAR SYSTEM PERTURBED BY TERM WITH LINEAR SPATIAL DEPENDENCE

Consider an ODE system of the form:

$$\frac{\mathrm{d}\boldsymbol{y}}{\mathrm{d}t} = \boldsymbol{G}(\boldsymbol{x}, \boldsymbol{y}) = \boldsymbol{g}(\boldsymbol{y}) + \boldsymbol{H}(\boldsymbol{x})\boldsymbol{y} + \boldsymbol{h}(\boldsymbol{x}), \tag{A.1}$$

for $\boldsymbol{y} \in \mathbb{R}^{N_y}$ where $\boldsymbol{g} : \mathbb{R}^{N_y} \to \mathbb{R}^{N_y}$, $\boldsymbol{h} : \mathbb{R}^{N_x} \to \mathbb{R}^{N_y}$ and $\boldsymbol{H} : \mathbb{R}^{N_x} \to \mathbb{R}^{N_y} \times \mathbb{R}^{N_y}$ are arbitrary functions which may be nonlinear, and where $\boldsymbol{x} \in \mathbb{R}^{N_x}$ is vector of parameters. Consider a particular reference set of parameters $\boldsymbol{x} = \boldsymbol{\xi}$ for which $\phi^t \boldsymbol{y}$ is the flow map and μ_ξ is an ergodic invariant probability measure. Let $\overline{\boldsymbol{H}}$ and $\overline{\boldsymbol{h}}$ be appropriate reference values of $\boldsymbol{H}(\boldsymbol{x})$ and $\boldsymbol{h}(\boldsymbol{x})$ and define $\delta\boldsymbol{H}(\boldsymbol{x}) := \boldsymbol{H}(\boldsymbol{x}) - \overline{\boldsymbol{H}}$ and $\delta\boldsymbol{h}(\boldsymbol{x}) := \boldsymbol{h}(\boldsymbol{x}) - \overline{\boldsymbol{h}}$. We can then rewrite the RHS of (Equation A.1) as

$$\boldsymbol{G}(\boldsymbol{x}, \boldsymbol{z}) = \boldsymbol{g}(\boldsymbol{z}) + (\overline{\boldsymbol{H}} + \delta\boldsymbol{H}(\boldsymbol{x}))\boldsymbol{z} + (\overline{\boldsymbol{h}} + \delta\boldsymbol{h}(\boldsymbol{x})). \tag{A.2}$$

In the case where $\delta\boldsymbol{H} = \delta\boldsymbol{h} = 0$, let $\overline{\boldsymbol{z}}_\xi$ and Σ_ξ be the mean and mean-centered covariance for this system. Then we can rewrite (Equation A.2) as

$$\boldsymbol{G}(\boldsymbol{x}, \boldsymbol{z}) = \boldsymbol{g}(\boldsymbol{z}) + \overline{\boldsymbol{H}}\boldsymbol{z} + \overline{\boldsymbol{h}} + \delta\boldsymbol{G}(\boldsymbol{x}, \boldsymbol{z}), \tag{A.3}$$

Appendix A (Continued)

where

$$\begin{aligned}\delta \boldsymbol{G}(\boldsymbol{x}, \boldsymbol{z}) &= \delta \boldsymbol{H}(\boldsymbol{x})\boldsymbol{z} + \delta \boldsymbol{h}(\boldsymbol{x}) \\ &= \delta \boldsymbol{H}(\boldsymbol{x})(\boldsymbol{z} - \overline{\boldsymbol{z}}_\xi) + \delta \boldsymbol{h}(\boldsymbol{x}) + \delta \boldsymbol{H}(\boldsymbol{x})\overline{\boldsymbol{z}}_\xi\end{aligned} \tag{A.4}$$

is a linear function in $\boldsymbol{z}$. Now we are interested in the responses of $\overline{\boldsymbol{z}}_\xi$ and Σ_ξ to changes in $\delta \boldsymbol{G}(\boldsymbol{x}, \boldsymbol{z})$. For a differentiable scalar function $b(\boldsymbol{z})$ with average state $\langle b \rangle = \int b(\boldsymbol{z})\, \mathrm{d}\mu_\xi(\boldsymbol{z})$, recall the response formula (Equation 3.23):

$$\begin{aligned}\delta\langle b \rangle(t) &= \int_0^t \int \nabla_z \left(b(\phi^{t-\tau}\boldsymbol{z}) \right) \delta \boldsymbol{G}(\boldsymbol{x}, \boldsymbol{z})\, \mathrm{d}\mu_\xi(\boldsymbol{z})\, \mathrm{d}\tau \\ &= \int_0^t \int \nabla_z \left(b(\phi^{\tau}\boldsymbol{z}) \right) \delta \boldsymbol{G}(\boldsymbol{x}, \boldsymbol{z})\, \mathrm{d}\mu_\xi(\boldsymbol{z})\, \mathrm{d}\tau \\ &= \int_0^t \int \nabla_z \left(b(\phi^{\tau}\boldsymbol{z}) - \langle b \rangle \right) \delta \boldsymbol{G}(\boldsymbol{x}, \boldsymbol{z})\, \mathrm{d}\mu_\xi(\boldsymbol{z})\, \mathrm{d}\tau.\end{aligned} \tag{A.5}$$

Suppose μ_ξ is absolutely continuous with respect to the Lebesgue measure with distribution density $\rho_\xi(\boldsymbol{y}) = e^{-q_\xi(\boldsymbol{y})}$, where q is a differentiable function that goes to infinity as $|\boldsymbol{x}| \to \infty$. Integrating by parts gives us

$$\begin{aligned}\delta\langle b \rangle(t) &= -\int_0^t \int \left(b(\phi^{\tau}\boldsymbol{z}) - \langle b \rangle \right) \nabla_x \cdot \left(\delta \boldsymbol{G}(\boldsymbol{x}, \boldsymbol{z}) \rho_\xi(\boldsymbol{z}) \right)\, \mathrm{d}\boldsymbol{z}\, \mathrm{d}\tau \\ &= -\int_0^t \int \left(b(\phi^{\tau}\boldsymbol{z}) - \langle b \rangle \right) \nabla_x \cdot \left(\delta \boldsymbol{G}(\boldsymbol{x}, \boldsymbol{z}) e^{-q_\xi(\boldsymbol{z})} \right)\, \mathrm{d}\boldsymbol{z}\, \mathrm{d}\tau \\ &= \int_0^t \int \left(b(\phi^{\tau}\boldsymbol{z}) - \langle b \rangle \right) \left(\nabla_x q_\xi(\boldsymbol{z}) \cdot \delta \boldsymbol{G}(\boldsymbol{x}, \boldsymbol{z}) - \nabla_x \cdot \delta \boldsymbol{G}(\boldsymbol{x}, \boldsymbol{z}) \right)\, \mathrm{d}\mu_\xi(\boldsymbol{z})\, \mathrm{d}\tau.\end{aligned} \tag{A.6}$$

Since $\nabla_x \cdot \delta \boldsymbol{G}(\boldsymbol{x}, \boldsymbol{z}) = \delta \boldsymbol{H}(\boldsymbol{x})$ is a constant, we have

$$\delta\langle b \rangle(t) = \int_0^t \int \left(b(\phi^{\tau}\boldsymbol{z}) - \langle b \rangle \right) \left(\nabla_x q_\xi(\boldsymbol{z}) \cdot \delta \boldsymbol{G}(\boldsymbol{x}, \boldsymbol{z}) \right)\, \mathrm{d}\mu_\xi(\boldsymbol{z})\, \mathrm{d}\tau. \tag{A.7}$$

Appendix A (Continued)

For an ergodic system we switch to a time average, and expanding the forcing term $\delta \boldsymbol{G}$ we have

$$\begin{aligned}\delta\langle b\rangle(t) = &\lim_{S\to\infty}\frac{1}{S}\int_0^t\int_0^S (b(\boldsymbol{z}(s+\tau)) - \langle b\rangle)\left((\Sigma_\xi^{-1})(\boldsymbol{z}(s)-\overline{\boldsymbol{z}}_\xi)\right)^T \delta\boldsymbol{H}(\boldsymbol{x})(\boldsymbol{z}(s)-\overline{\boldsymbol{z}}_\xi)\,\mathrm{d}s\,\mathrm{d}\tau \\ &+\lim_{S\to\infty}\frac{1}{S}\int_0^t\int_0^S (b(\boldsymbol{z}(s+\tau)) - \langle b\rangle)(\boldsymbol{z}(s)-\overline{\boldsymbol{z}}_\xi)^T\,\mathrm{d}s\,\mathrm{d}\tau\,(\Sigma_\xi^{-1})\left(\delta\boldsymbol{h}(\boldsymbol{x})+\delta\boldsymbol{H}(\boldsymbol{x})\overline{\boldsymbol{z}}_\xi\right).\end{aligned} \tag{A.8}$$

Using the identity $\boldsymbol{u}^T A\boldsymbol{v} = \boldsymbol{u}\boldsymbol{v}^T : A$, where : is the Frobenius (component-wise) inner product, we have

$$\begin{aligned}\delta\langle b\rangle(t) = &\lim_{S\to\infty}\frac{1}{S}\int_0^t\int_0^S (b(\boldsymbol{z}(s+\tau)) - \langle b\rangle)(\boldsymbol{z}(s)-\overline{\boldsymbol{z}}_\xi)(\boldsymbol{z}(s)-\overline{\boldsymbol{z}}_\xi)^T\,\mathrm{d}s\,\mathrm{d}\tau\,(\Sigma_\xi^{-1}) : \delta\boldsymbol{H}(\boldsymbol{x}) \\ &+\lim_{S\to\infty}\frac{1}{S}\int_0^t\int_0^S b(\boldsymbol{z}(s+\tau))(\boldsymbol{z}(s)-\overline{\boldsymbol{z}}_\xi)^T\,\mathrm{d}s\,\mathrm{d}\tau\,(\Sigma_\xi^{-1})\left(\delta\boldsymbol{h}(\boldsymbol{x})+\delta\boldsymbol{H}(\boldsymbol{x})\overline{\boldsymbol{z}}_\xi\right).\end{aligned} \tag{A.9}$$

CITED LITERATURE

1. Young, L.-S.: What are srb measures, and which dynamical systems have them? Journal of Statistical Physics, 108(5):733–754, 2002.

2. Abramov, R. V.: Linear response of the lyapunov exponent to a small constant perturbation. arXiv preprint, arXiv:1403.7116v1 [math.DS], 2014.

3. Einstein, A.: ber die von der molekularkinetischen theorie der wrme geforderte bewegung von in ruhenden flssigkeiten suspendierten teilchen. Annalen der Physik, 322(8):549–560, 1905.

4. von Smoluchowski, M.: Zur kinetischen theorie der brownschen molekularbewegung und der suspensionen. Annalen der Physik, 326(14):756–780, 1906.

5. Kubo, R.: The fluctuation-dissipation theorem. Reports on progress in physics, 29(1):255, 1966.

6. Marconi, U. M. B., Puglisi, A., Rondoni, L., and Vulpiani, A.: Fluctuation–dissipation: response theory in statistical physics. Physics reports, 461(4):111–195, 2008.

7. Nyquist, H.: Thermal agitation of electric charge in conductors. Phys. Rev., 32:110–113, Jul 1928.

8. Callen, H. B. and Welton, T. A.: Irreversibility and generalized noise. Physical Review, 83(1):34, 1951.

9. Kubo, R.: Statistical-mechanical theory of irreversible processes. i. general theory and simple applications to magnetic and conduction problems. Journal of the Physical Society of Japan, 12(6):570–586, 1957.

10. Kraichnan, R. H.: Classical fluctuation-relaxation theorem. Physical Review, 113(5):1181, 1959.

11. Leith, C. E.: Climate response and fluctuation dissipation. Journal of the Atmospheric Sciences, 32(10):2022–2026, 1975.

12. Leith, C. E.: Predictability of climate. Nature, 276:352–355, 1978.

13. Deker, U. and Haake, F.: Fluctuation-dissipation theorems for classical processes. Physical Review A, 11(6):2043, 1975.

14. Risken, H.: Fokker-Planck Equation. Springer, 1984.

15. Majda, A., Abramov, R. V., and Grote, M. J.: Information theory and stochastics for multiscale nonlinear systems, volume 25 of Center for Research in Mathematics Monograph Series. American Mathematical Soc., 2005.

16. Ruelle, D.: Chaotic evolution and strange attractors, volume 1. Cambridge University Press, 1989.

17. Ruelle, D.: Differentiation of srb states. Communications in Mathematical Physics, 187(1):227–241, 1997.

18. Zeeman, E. C.: Stability of dynamical systems. Nonlinearity, 1(1):115, 1988.

19. Abramov, R. V.: Short-time linear response with reduced-rank tangent map. Chinese Annals of Mathematics, Series B, 30(5):447–462, 2009.

20. Abramov, R. V.: Approximate linear response for slow variables of dynamics with explicit time scale separation. Journal of Computational Physics, 229(20):7739–7746, 2010.

21. Abramov, R. V.: Improved linear response for stochastically driven systems. Frontiers of Mathematics in China, 7(2):199–216, 2012.

22. Abramov, R. V. and Majda, A. J.: New approximations and tests of linear fluctuation-response for chaotic nonlinear forced-dissipative dynamical systems. Journal of Nonlinear Science, 18(3):303–341, 2008.

23. Abramov, R. V. and Majda, A. J.: Blended response algorithms for linear fluctuation-dissipation for complex nonlinear dynamical systems. Nonlinearity, 20(12):2793, 2007.

24. Ruelle, D.: General linear response formula in statistical mechanics, and the fluctuation-dissipation theorem far from equilibrium. Physics Letters A, 245(3):220–224, 1998.

25. Gritsun, A. and Branstator, G.: Climate response using a three-dimensional operator based on the fluctuation-dissipation theorem. Journal of the atmospheric sciences, 64(7):2558–2575, 2007.

26. Bell, T. L.: Climate sensitivity from fluctuation dissipation: Some simple model tests. Journal of the Atmospheric Sciences, 37(8):1700–1707, 1980.

27. Langen, P. L. and Alexeev, V. A.: Estimating 2× co2 warming in an aquaplanet gcm using the fluctuation-dissipation theorem. Geophysical research letters, 32(23), 2005.

28. Pavliotis, G. and Stuart, A.: Multiscale methods: averaging and homogenization, volume 53 of Texts in Applied Mathematics. Springer, 2008.

29. Bender, C. M. and Orszag, S. A.: Advanced Mathematical Methods for Scientists and Engineers I. Springer Science & Business Media, 1999.

30. Bensoussan, A., Lions, J.-L., and Papanicolaou, G.: Asymptotic analysis for periodic structures, volume 374. American Mathematical Soc., 2011.

31. Volosov, V. M.: Averaging in systems of ordinary differential equations. Russian Mathematical Surveys, 17(6):1–126, 1962.

32. Givon, D., Kupferman, R., and Stuart, A.: Extracting macroscopic dynamics: model problems and algorithms. Nonlinearity, 17(6):R55, 2004.

33. Abramov, R. V.: A simple linear response closure approximation for slow dynamics of a multiscale system with linear coupling. Multiscale Modeling & Simulation, 10(1):28–47, 2012.

34. Abramov, R. V. and Kjerland, M. P.: The response of reduced models of multiscale dynamics to small external perturbations. arXiv preprint, arXiv:1305.0862 [math.DS], 2013.

35. Lorenz, E. N.: Predictability: A problem partly solved. In Proc. Seminar on predictability, ECMWF, volume 1, 1996.

36. Abramov, R. V.: Suppression of chaos at slow variables by rapidly mixing fast dynamics through linear energy-preserving coupling. Communications in Mathematical Sciences, 10(2), 2012.

37. Abramov, R. V.: A simple closure approximation for slow dynamics of a multiscale system: nonlinear and multiplicative coupling. Multiscale Modeling & Simulation, 11(1):134–151, 2013.

38. Lin, J.: Divergence measures based on the shannon entropy. Information Theory, IEEE Transactions on, 37(1):145–151, 1991.

39. Kullback, S. and Leibler, R. A.: On information and sufficiency. The Annals of Mathematical Statistics, pages 79–86, 1951.

40. Rubner, Y., Tomasi, C., and Guibas, L. J.: The earth mover's distance as a metric for image retrieval. International Journal of Computer Vision, 40(2):99–121, 2000.

41. Abdi, H.: Partial least squares regression, 2003.

42. Gritsun, A. and Dymnikov, V.: Barotropic atmosphere response to small external actions: Theory and numerical experiments. Izvestiia-Russian Academy Of Sciences Atmospheric And Oceanic Physics C/C Of Izvestiia-Rossiiskaia Akademiia Nauk Fizika Atmosfery I Okeana, 35:511–525, 1999.

43. Abramov, R. V. and Majda, A. J.: A new algorithm for low-frequency climate response. Journal of the Atmospheric Sciences, 66(2):286–309, 2009.

44. Abramov, R. V. and Majda, A. J.: Low-frequency climate response of quasigeostrophic wind-driven ocean circulation. Journal of Physical Oceanography, 42(2):243–260, 2012.

45. Abramov, R. V.: A simple stochastic parameterization for reduced models of multiscale dynamics. arXiv preprint, arXiv:1302.4132 [math.DS], 2013.

46. Onsager, L.: Reciprocal relations in irreversible processes. i. Physical Review, 37(4):405, 1931.